ISMRM ONE COMMUNITY FOR CLINICIANS AND SCIENTISTS

NUKEM Isotopes

ISMRM 2017 NEWSLETTER

NUKEM Isotopes Imaging GmbH

Oxygen-17 ISMRM Abstracts

MR-Bibliography about Oxygen-17

Product Brochures

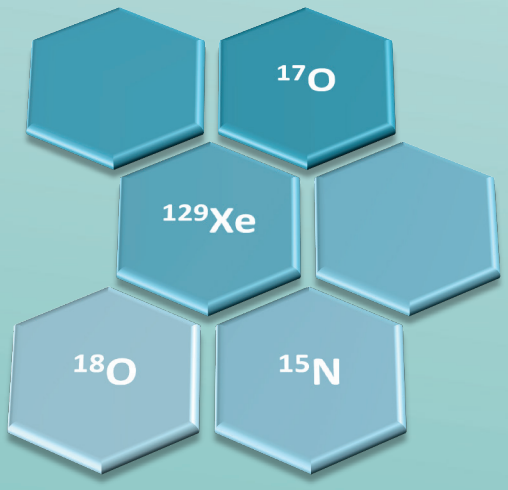

Contact us

www.nukem-isotopes.com

Company information

NUKEM Isotopes GmbH based in Alzenau, Germany is a global leader in providing isotopes in the form of ultra-pure substances for industry, agriculture and medical applications. We have been a reliable partner for long term demands of stable isotopes for more than two decades. We maintain our partnership with the major enrichment enterprises in the Peoples Republic of China, the Republic of Georgia and the Russian Federation. With our warehouses at Frankfurt Airport, Hamburg seaport and cooperation partners in USA, we are able to ship our isotopes within 48 hours to our clients worldwide. With our quality management (ISO 9001-2008, NUPIC) as well as third party analysis of our products, we guarantee our customers reliable services and high quality isotopes.

NUKEM Isotopes Imaging GmbH was established in 2015 and is specialized in the supply of stable isotopes, which are used in the field of Magnetic Resonance Imaging (MRI). Currently NUKEM Isotopes Imaging GmbH provides two isotopes, Oxygen-17 and Xenon-129, in different forms and enrichments. For further information, please check the following pages, visit our website (www.nukem-isotopes.com) or contact us directly (ISMRM 2017, booth no.: 222). NUKEM Isotopes Imaging GmbH is ISO 9001-2008 certified and has established long term relationships with medical companies, who are specialized in producing ultra-pure products in compliance with cGMP regulations. This guarantees our customers in the medical fields a high quality and safe product.

Oxygen-17 in the form of Oxygen gas

NMR technology based on Oxygen-17 uses the magnetic properties of atomic nuclei that occur naturally in the body. Oxygen-17 (^{17}O) is now being used for diagnostic applications and medical research to create a new generation of NMR Images.

New developments with ^{17}O enhance the quality of information about living tissue to improve the practice of medicine in the fields of cardiology and neurology among others.

The magnetic property of ^{17}O makes it to a promising tool for assessing in vivo metabolic tissue information at high fields (≥3T).

The latest research results, performed with our 70at% enriched ^{17}O gas can be found on the following pages (p.3-6).

Enrichment	^{17}O > 70at%
Purity	> 99.9%
Volume	5L, 10L and 20L with a CGA 540 valve (left picture). 1L and 2L with a ¼" NPT valve (right picture)

CO	≤ 10 ppm
CO_2	≤ 100 ppm
H_2	≤ 50 ppm
N_2	≤ 500 ppm

Our Oxygen-17 products are manufactured in accordance with cGMP regulations and with the requirements of 21 Code of Federal Regulations: PARTS 210 and 211.

ISMRM-Abstract (^{17}O in the form of gas)

Direct Partial Volume Corrected $CMRO_2$ Determination: Simulation Assisted Dynamic ^{17}O-MRI

Sebastian C. Niesporek[1], Reiner Umathum[1], Jonathan M. Lommen[1] and Armin M. Nagel[1,2]

[1]Medical Physics in Radiology, German Cancer Research Center (DKFZ), Heidelberg, Germany,[2]Institute of Radiology, University Hospital Erlangen, Erlangen, Germany

PURPOSE The oxygen metabolism (oxidative phosphorylation) in the human brain is an indicator of cell viability. The only stable MR-visible oxygen isotope (^{17}O, nat. abundance 0.037%) can be utilized in a dynamic inhalation experiment for a localized determination of the cerebral metabolic rate of oxygen consumption ($CMRO_2$) by quantification of $H_2{}^{17}O$[1]. A changing $CMRO_2$-value can for example be seen in tumor cells[2] ('Warburg Effect') or in Alzheimer's disease[3]. Therefore, an accurate and localized $CMRO_2$-determination is of interest to study the metabolism under various conditions or for treatment evaluation. Quantification accuracy of ^{17}O-MRI is severely limited by partial volume (PV) effects, that are caused by fast T_2^*-relaxation and low spatial resolution of ((5-10mm)^3). Latter is caused by a factor of 10^6 reduced in-vivo ^{17}O-signal compared to protons. Therefore, pulse sequences that enable ultra-short echo-times and high SNR-efficiency such as 3D-density-adapted radial (3D-DAPR)[4] or twisted-projection imaging[5] are used. For quantification in non-proton MRI, a partial volume correction (PVC) algorithm[6] was already successfully applied[7,8]. In the presented study a dynamic ^{17}O-inhalation experiment of a healthy volunteer was conducted. Effects of temporal resolution, a sliding-window-reconstruction (SWR) technique and PVC were evaluated by simulation and findings were applied to experimental data.

METHODS An in-house developed human brain-simulation was modified for simulation of dynamic signal evolution, analogous to an inhalation experiment (Fig.1A). Tissue water-concentration[9] (c_W) was simulated as follows: GM-c_W =80% and $CMRO_2$=2.0µmol/g*min; WM-c_W=69% and $CMRO_2$=0.7µmol/g*min and CSF-c_W =100% (no metabolism). Dynamic ^{17}O-data was reconstructed with variable temporal resolution Δt (Δt=0:30min-2:00min) and PVC was applied to every data-set for quantification of $H_2{}^{17}O$. Three compartments (CSF, grey (GM) and white matter (WM)) were considered and T2*-decay[10] was incorporated into simulation and correction. A three-phase metabolic model[1] was fitted to corrected data to obtain $CMRO_2$-values in considered brain compartments.
For the in-vivo experiment a MR-compatible breathing-system, administering a variable ^{17}O-bolus in a closed circuit (Fig.1A), was used. Imaging was conducted with a custom-built $^{17}O/^{1}H$-head-coil on a 7T MR-system[11]. ^{17}O-data was acquired with a 3D-DAPR-sequence using a Golden-Angle (GA) projection acquisition-scheme[12] allowing variable Δt with a nominal spatial resolution of (7.5mm)^3 (Fig.1B). During the three-phase-experiment (T_{Acq}=40:00min), 4.0±0.1L of 70%-enriched ^{17}O-gas[13] was inhaled by a male volunteer (age 65): baseline-phase (10:00min, room-air), ^{17}O-inhalation phase (11:30min), decay phase (17:30min, room-air). Additional data for B1-correction[14] and anatomical ^{1}H-data were acquired as registration- and segmentation-basis. Post-processing of measured data-sets was conducted analogous to simulations.

RESULTS Quantification results were verified with the simulation's ground-truth (GT): PV-corrected data, with and without simulated noise showed deviation of c_W of 1-8% for GM and 0-5% for WM. In contrast, 25-32% for GM and 11-16% for WM was observed for non-corrected data, respectively. PV-bias was also seen for pre-PVC $CMRO_2$-values determined before PVC. The PVC showed improvement with minor influence on chosen Δt (Tab.1/Fig.2) for GM and WM.
Obtained c_W-values for PV-corrected experimental data in the baseline-phase was within ±5% of expected value for all considered compartments. The enrichment-factor α of administered ^{17}O-gas in the breathing-system was estimated to 49±3% and determined $CMRO_2$ values were: $CMRO_2$=2.07±0.15µmol/g*min (GM) and

$CMRO_2$=0.65±0.03µmol/g*min (WM) (Tab.2/Fig.3). A SWR where consecutive reconstruction timeframes were shifted backward by Δt/2 was also applied and evaluated in simulations and also adopted to in-vivo data (Tab.1B/Tab.2), showing no change in obtained $CMRO_2$.

DISCUSSION Utilization of the brain-simulation allowed direct verification of dynamic ^{17}O-data analysis in a realistic setting: strong PV-influence was seen for $H_2{}^{17}O$-concentration and $CMRO_2$-values (19-55%) which led to over- and underestimation of the metabolic rate. The applied PVC is able to correct close to the GT by decreasing the PV-bias on $CMRO_2$-values (max. deviation 8.5%). The GA-acquisition allowed evaluation of a variable Δt and the SWR: $CMRO_2$-values showed negligible influence on chosen Δt and SWR, whereas application of a SWR reduced fitting errors. Inaccuracies in quantification and fitting uncertainty are mainly influenced by decreasing SNR with lower Δt.
The in-vivo data exhibited similar behavior for varying Δt and SWR. WM $CMRO_2$-values (lowest expected PV-bias) are in good agreement with other studies[1,7,15,16] (Tab.2) whereas GM $CMRO_2$-values show more variation: Studies without PVC state an up to 30% lower GM-CMRO2-value. However, in-vivo GM- and WM baseline-c_W is still underestimated by 4-6%, most likely due to not fully corrected transverse relaxation which can also slightly influence determined $CMRO_2$-values.

CONCLUSION The presented simulation-assisted dynamic ^{17}O-MRI experiment verifies the applied PVC-algorithm, improves $CMRO_2$-determination and optimizes post-processing. The ability to investigate Δt and applied SWR helps to save expensive ^{17}O-gas. This approach will be pursued in further inhalation measurements aiming to show reproducibility in volunteer studies. Furthermore, our breathing system has a low breathing resistance allowing patient measurements.

REFERENCES

[1] Atkinson et al., Neuroimage 2010 (51): 723–733, [2] Miles KA, Williams RE., Cancer Imaging 2008 (8):81-86, [3] Beal MF., Ann Neurol; 1992 (2):119-130, [4] Nagel et al*., Magn Reson Med 2009 (62):1565-73,* [5] Boada et al., *Magn Reson Med (1997); 37: p. 706-715,* [6] Rousset et al., *J Nucl Med 1998(5):904-911, 1998,* [7] Hoffmann et al*., MAGMA 2014(27):579-87,* [8] Niesporek et al., *NeuroImage, 2015(112): 353–363,*[9] Neeb et al., *NeuroImage, 2006 (31): 1156–1168,* [10] *Niesporek et al., Proc. ISMRM 24 (2016, #3964),* [11] Magnetom 7T, Siemens AG, Erlangen, Germany, [12] Chan, R.W. et al., *Magn Reson Med 2009(61): p. 354–363,* [13] NUKEM Isotopes Imaging GmbH, Alzenau, Germany, [14] Morell*, Magn Reson Med 2008 (60):889-94,* [15] *Hoffmann et al., Magn Reson Med; 66:1109-15 (2011),* [16] *Borowiak et al., Proc. ISMRM 23 (2015, #4633)*

Review category (proposal):
603 MRS: Non-proton MRS and MRI (all nuclei) - Methods & Applications
705 Molecular Imaging: Other (Original Research, Not Education)

SYNOPSIS A dynamic ^{17}O-MRI inhalation experiment enables localized mapping of the cerebral metabolic rate of oxygen consumption ($CMRO_2$) in the human brain via $H_2{}^{17}O$ quantification. These functional information are tissue viability parameters and can help studying the brain metabolism. In ^{17}O-MRI accurate quantification and $CMRO_2$-determination is severely biased by partial volume effects caused by low spatial resolution and fast transverse relaxation. A human brain-simulation providing realistic dynamic ^{17}O-data was used to evaluate the performance of a partial volume correction algorithm at different temporal resolution. Findings were then adapted to an in-vivo ^{17}O-MRI inhalation experiment which was conducted in a healthy volunteer.

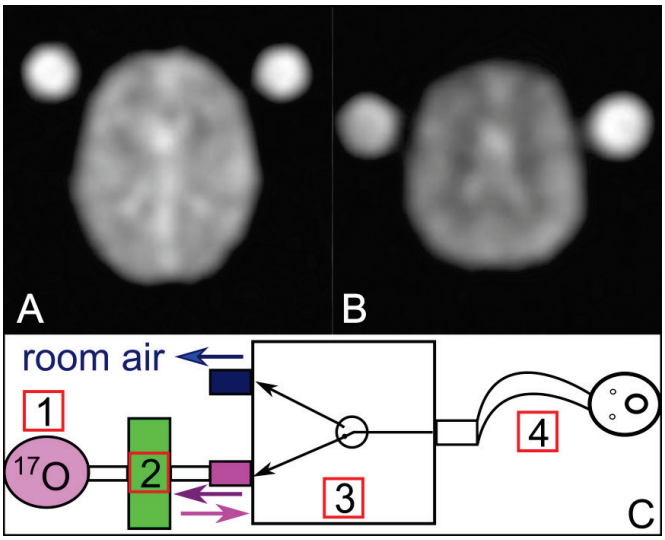

Fig. 1 *Simulated ^{17}O-baseline image* ***(A)*** *and measured ^{17}O-baseline image (no B1-correction)* ***(B)*** *acquired with a 3D-DARP-sequence (TR/TE=20/0.56ms, Θ=60°, Golden-Angle acquisition, Δt=2min). Sketch showing the utilized breathing-system* ***(C)*** *consisting of a ^{17}O-reservoir (1), CO_2-absorber (2), remote controllable pneumatic valve (3) switching between room air and closed ^{17}O-breathing circuit and non-vented breathing mask (4).*

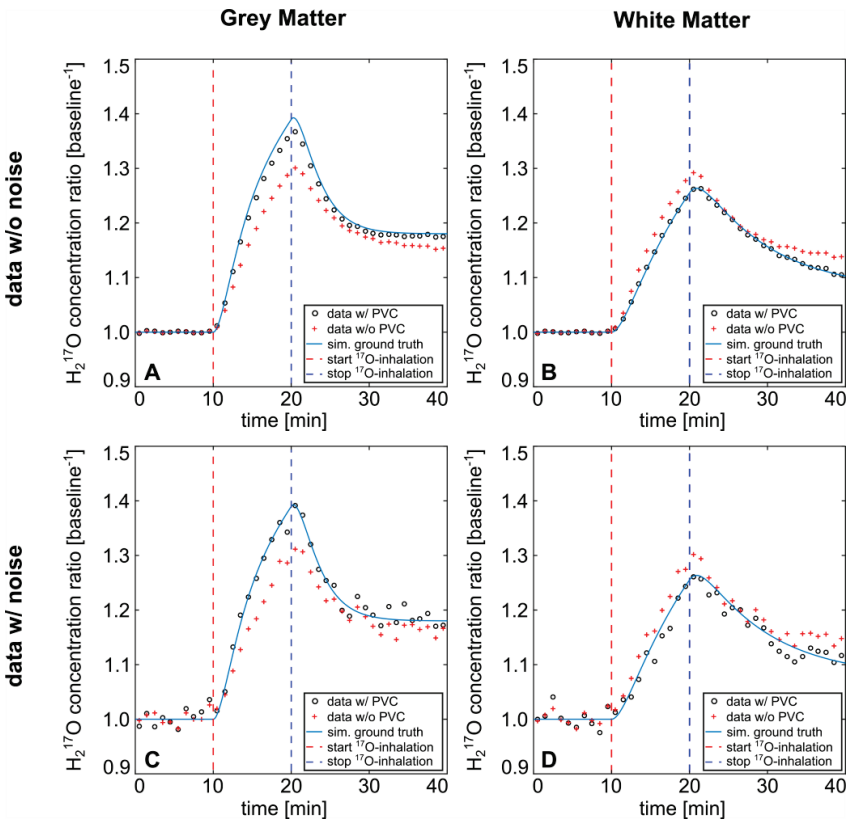

Fig. 2 *Representative fits of the evolution of tissue $H_2{}^{17}O$ concentration during a simulated inhalation experiment with Δt=1min without (A,B) and with considered noise (C,D) for grey matter (A,C) and white matter (B,D). Start and stop of simulated ^{17}O-inhalation is indicated by dashed lines. A maximal signal increase of ~40% is seen. The data is normalized to the baseline-concentration to enable better visualization of the PV-bias. Quantification was determined with (black circles) and without (red crosses) PVC and compared to the simulated ground truth (solid line). PV-bias is leading to an underestimation of $CMRO_2$-values of up to 55%.*

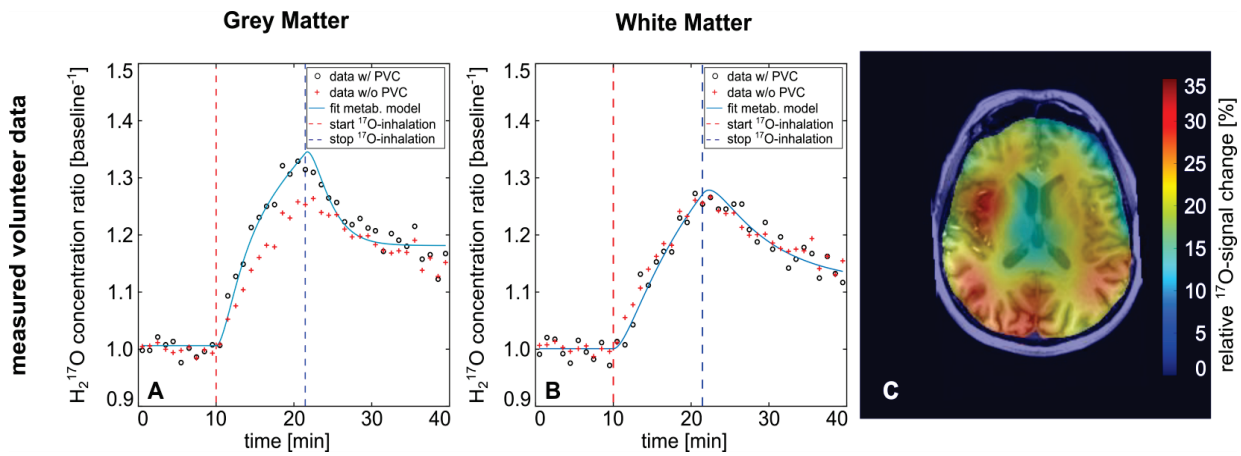

Fig. 3 Representative fits of the evolution of tissue $H_2{}^{17}O$-concentration during an in-vivo inhalation experiment of male volunteer (age 65) with Δt=1min for grey matter (A), white matter (B) and map of relative ^{17}O-signal increase with anatomical overlay (C). Start and stop of ^{17}O-inhalation (duration 11:30min, 4.0 ±0.1L of ^{17}O-gas) are indicated by dashed lines and a maximal signal increase of ~35% is seen. The data was normalized to the baseline-concentration for better visualization of PV-bias. Quantification was determined with (red circles) and without (black crosses) PVC and a 3-phase metabolic model were fitted to data with PVC (solid line).

Oxygen-17 in the form of glucose

As the first company in the world, we synthesised substantial amounts of single and double labelled O-17 D-Glucose and in cooperation with different research institutes, we performed the first in vivo tests with Oxygen-17 labeled Glucose.

The latest research results about the application of O-17 enriched D-Glucose can be found on the following pages (p.7-14).

Enrichment	^{17}O ≈ 38at% at position 6 only
Purity	> 99.9%

If you are interested in other enrichments (also labelled at other positions of the glucose) or in other molecules, labelled with Oxygen-17, please do not hesitate to contact us.

ISMRM-Abstract (^{17}O in the form of glucose)

Quantification of Cerebral Metabolic Rates of ^{17}O-Labeled Glucose in Mouse Brain with Dynamic ^{17}O-MRS

Robert Borowiak[1,2,3,4], Wilfried Reichardt[1,2,3,4], Dmitry Kurzhunov[1,2], Christian Schuch[5], Dieter Leibfritz[6], Benjamin Görling[7], Jochen Leupold[1,2], Thomas Lange[1,2], Michael Bock[1,2]

[1]Medical Physics, Department of Radiology, Medical Center – University of Freiburg, Germany,[2]Faculty of Medicine, University of Freiburg, Germany, [3]German Cancer Consortium (DKTK), Heidelberg, Germany, [4]German Cancer Research Center (DKFZ), Heidelberg, Germany, [5]NUKEM Isotopes Imaging GmbH, Alzenau, Germany, [6]Faculty of Medicine, University of Tübingen, Germany, 7Bruker Biospin, Rheinstetten, Germany

SYNOPSIS We studied the chemical exchange kinetics of ^{17}O-labeled glucose at the C1 and the C6 position with dynamic ^{17}O-MRS. A profile likelihood analysis is performed to determine identifiability and confidence intervals of the metabolic rate CMR_{Glc}. The exchange experiments confirm that the C6-^{17}OH label is transferred via glycolysis exclusively by the enzyme enolase into the metabolic end product $H_2{}^{17}O$, while C1-^{17}OH ends up in water via direct hydrolysis as well as via glycolysis. From $H_2{}^{17}O$-concentration time-courses cerebral metabolic rates of CMR_{Glc} = 0.05-0.08 µmol/g/min are obtained which are in of the same order of magnitude as ^{18}F-FDG PET.

INTRODUCTION Malignant tumors predominately gain energy by anaerobic glycolysis [1]. Currently, the clinical gold standard to assess glucose metabolism is positron emission tomography (PET) which uses the radioactively labeled [^{18}F]-fluordeoxyglucose (FDG). Recently, we have performed dynamic ^{17}O-MRS of ^{17}O-labeled glucose for the first time to follow up glycolysis in mouse brain [2].
The purpose of this study was to further investigate the dynamics of glucose labeled with ^{17}O at the C1 (Glc-1, 68 % labeled) and the C6 position (Glc-6, 43 % labeled) *in vivo* using dynamic ^{17}O-MRS at ultra-high field. Two representative in vivo Glc-6 data sets were acquired as described in [2], and profile likelihood analysis (PL) was performed [3–6] to reliably determine metabolic rates of glucose consumption (CMR_{Glc}) from the recorded time dependent course of the $H_2{}^{17}O$ resonances using a pharmacokinetic model.

MATERIAL & METHODS The 1-OH group at the anomeric C1 carbon of glucose (Glc-1) undergoes a known temperature and pH-dependent and concentration-independent chemical exchange with unlabeled water in aqueous solution [7,8]. Under physiological conditions the OH-group at the C6 position (Glc-6) cannot be replaced via chemical exchange in aqueous solutions, and no enzyme-catalyzed reaction is reported in the literature to substitute the C6-OH group in mammalians. However, recently we could show [2] that the C6-OH label is transferred in the glycolytic downstream by the enzyme enolase into the metabolic end product $H_2{}^{17}O$ (Figure 1).

EXCHANGE MEASUREMENTS To corroborate exchange dynamics, in a phantom experiment two 55 mM aqueous solutions of Glc-1 and Glc-6 dissolved in phosphate-buffered saline PBS (pH = 7.4, Sigma Aldrich) were prepared. Dynamic ^{17}O-MRS was performed of the solutions with a 500 MHz spectrometer (Avance III 500, Bruker Biospin) over up to 200 min. Each spectrum was measured with an FID sequence at a body temperature (37°C) with the following parameters: 90°-pulse duration T_{pulse} = 21.5 µs, acquisition delay 10 µs, TE = 21 µs, TR = 50 ms, spectral band width BW = 31.25 kHz (461 ppm). Within the acquisition time of T_{acq} = 33 ms each FID was sampled with 2048 points and a dwell time of 16 µs. In total, 1024 FID signals were averaged per spectrum resulting in a measurement time of 1 min.

Model Fit and Profile Likelihood Analysis
With the exchange rates of the phantom experiments it was investigated whether CMR_{Glc} can be reliably determined from dynamic ^{17}O MRS data. For this, a pharmacokinetic model was used [9] that requires an input function with model parameters α and ρ. These parameters were estimated from glucose tolerance tests [10] in mice after intravenous injection of unlabeled glucose. A profile likelihood analysis was then performed to assess whether CMR_{Glc} can be determined reliably from the time course of the $H_2{}^{17}O$-resonances; for this, it was considered that 1mol Glc-6 is converted into 1mol $H_2{}^{17}O$ during glucose metabolism.

RESULTS & DISCUSSION In the dynamic Glc-6 experiment (Figure 2a) neither a signal increase of the $H_2{}^{17}O$-resonance nor a decrease of the 6-OH resonance is observed which proves that exchange of hydroxyl groups at C-6 is kinetically inhibited, whereas in the Glc-1 exchange experiment (Figure 2b,c) a signal increase of 3.5 % is observed within the measurement time of 200 min. Thus, the C6-OH label will show up in water *in vivo* via glycolysis exclusively, while C1-OH ends up in $H_2{}^{17}O$ via either direct hydrolysis or glycolysis. Moreover this result indicates that the *in vivo* conversion rate of Glc-1 into $H_2{}^{17}O$ due to chemical exchange with water in blood is expected to be less than the metabolic rate [2].
As described in [11], α was estimated to 0.32 from the Glc-6 enrichment k = 43 %, the baseline and maximum concentration of the blood sugar measurements. The exponential fit to the blood sugar measurement yielded ρ-values of 0.033 /0.031 min^{-1} (Figure 3). In the PL analysis CMR_{Glc} rates in the range of 0.05-0.08 µmol/g/min were obtained (Figure 5a,b) from the $H_2{}^{17}O$-concentration-time courses (Figure 4). Note that similar metabolic rates of CMR_{Glc} = 0.06 µmol/g/min are obtained using a simplified model as proposed in [12]. The deviations from the literature value 0.26 ± 0.10 µmol/g/min (^{18}F-FDG PET, mouse, 1.0 % isoflurane anaesthesia) [13] might be due to imperfections of the pharmacokinetic model and uncertainties of α and ρ-values.

OUTLOOK Although ^{17}O-labeled glucose is currently less cost-effective than enriched ^{13}C-glucose, oxygen-17 is a promising tracer to investigate novel metabolic pathways, which might provide enhanced sensitivity compared to established ^{13}C-MRS methods [14]. In a future step dynamic ^{17}O-MRS will be applied in a mouse model to monitor the glucose turnover in tumors.

References

[1] O. Warburg, On the origin of cancer cells, Science. 123 (1956) 309–314. doi:10.1126/science.123.3191.309.
[2] Borowiak Robert, Reichardt Wilfried, Kurzhunov Dmitry, Schuch Christian, Jochen Leupold, Thomas Lange, Marco Reisert, Axel Krafft, Elmar Fischer, Michael Bock, Initial investigation of glucose metabolism in mouse brain using ^{17}O-glucose and dynamic ^{17}O-MRS, In proceedings of 24rd Annunal Meeting ISMRM (2015).
[3] D. Kurzhunov, R. Borowiak, H. Hass, P. Wagner, A.J. Krafft, J. Timmer, M. Bock, Quantification of oxygen metabolic rates in Human brain with dynamic ^{17}O MRI: Profile likelihood analysis, Magn. Reson. Med. (n.d.) n/a-n/a. doi:10.1002/mrm.26476.
[4] A. Raue, C. Kreutz, T. Maiwald, J. Bachmann, M. Schilling, U. Klingmüller, J. Timmer, Structural and practical identifiability analysis of partially observed dynamical models by exploiting the profile likelihood, Bioinformatics. 25 (2009) 1923–1929. doi:10.1093/bioinformatics/btp358.
[5] A. Raue, B. Steiert, M. Schelker, C. Kreutz, T. Maiwald, H. Hass, J. Vanlier, C. Tönsing, L. Adlung, R. Engesser, W. Mader, T. Heinemann, J. Hasenauer, M. Schilling, T. Höfer, E. Klipp, F. Theis, U. Klingmüller, B. Schöberl, J. Timmer, Data2Dynamics: a modeling environment tailored to parameter estimation in dynamical systems, Bioinformatics. 31 (2015) 3558–3560. doi:10.1093/bioinformatics/btv405.

[6] A.C. Hindmarsh, P.N. Brown, K.E. Grant, S.L. Lee, R. Serban, D.E. Shumaker, C.S. Woodward, SUNDIALS: Suite of nonlinear and differential/algebraic equation solvers, ACM Trans Math Softw. 31 (2005) 363–396. doi:10.1145/1089014.1089020.
[7] J.M. Risley, R.L. Van Etten, Kinetics of oxygen exchange at the anomeric carbon atom of D-glucose and D-erythrose using the oxygen-18 isotope effect in carbon-13 nuclear magnetic resonance spectroscopy, Biochemistry (Mosc.). 21 (1982) 6360–6365. doi:10.1021/bi00268a007.
[8] T.L. Mega, S. Cortes, R.L. Van Etten, The oxygen-18 isotope shift in carbon-13 nuclear magnetic resonance spectroscopy. 13. oxygen exchange at the anomeric carbon of D-glucose, D-mannose, and D-fructose, J. Org. Chem. 55 (1990) 522–528. doi:10.1021/jo00289a026.
[9] I.C. Atkinson, K.R. Thulborn, Feasibility of mapping the tissue mass corrected bioscale of cerebral metabolic rate of oxygen consumption using 17-oxygen and 23-sodium MR imaging in a human brain at 9.4 T, NeuroImage. 51 (2010) 723–733. doi:10.1016/j.neuroimage.2010.02.056.
[10] S. Andrikopoulos, A.R. Blair, N. Deluca, B.C. Fam, J. Proietto, Evaluating the glucose tolerance test in mice, Am. J. Physiol. - Endocrinol. Metab. 295 (2008) E1323–E1332. doi:10.1152/ajpendo.90617.2008.
[11] S.M. Fitzpatrick, H.P. Hetherington, K.L. Behar, R.G. Shulman, The flux from glucose to glutamate in the rat brain in vivo as determined by ^{1}H-observed, ^{13}C-edited NMR spectroscopy, J. Cereb. Blood Flow Metab. 10 (1990) 170–179. doi:10.1038/jcbfm.1990.32.
[12] N. Zhang, X.-H. Zhu, H. Lei, K. Ugurbil, W. Chen, Simplified Methods for Calculating Cerebral Metabolic Rate of Oxygen Based on ^{17}O Magnetic Resonance Spectroscopic Imaging Measurement during a Short $^{17}O_2$ Inhalation, J. Cereb. Blood Flow Metab. 24 (2004) 840–848. doi:10.1097/01.WCB.0000125885.54676.82.
[13] H. Toyama, M. Ichise, J.-S. Liow, K.J. Modell, D.C. Vines, T. Esaki, M. Cook, J. Seidel, L. Sokoloff, M.V. Green, R.B. Innis, Absolute quantification of regional cerebral glucose utilization in mice by ^{18}F-FDG small animal PET scanning and 2-14C-DG autoradiography, J. Nucl. Med. 45 (2004) 1398–1405.
[14] R.A. de Graaf, P.B. Brown, D.L. Rothman, K.L. Behar, Natural abundance ^{17}O NMR spectroscopy of rat brain in vivo, J. Magn. Reson. 193 (2008) 63–67. doi:10.1016/j.jmr.2008.04.019.

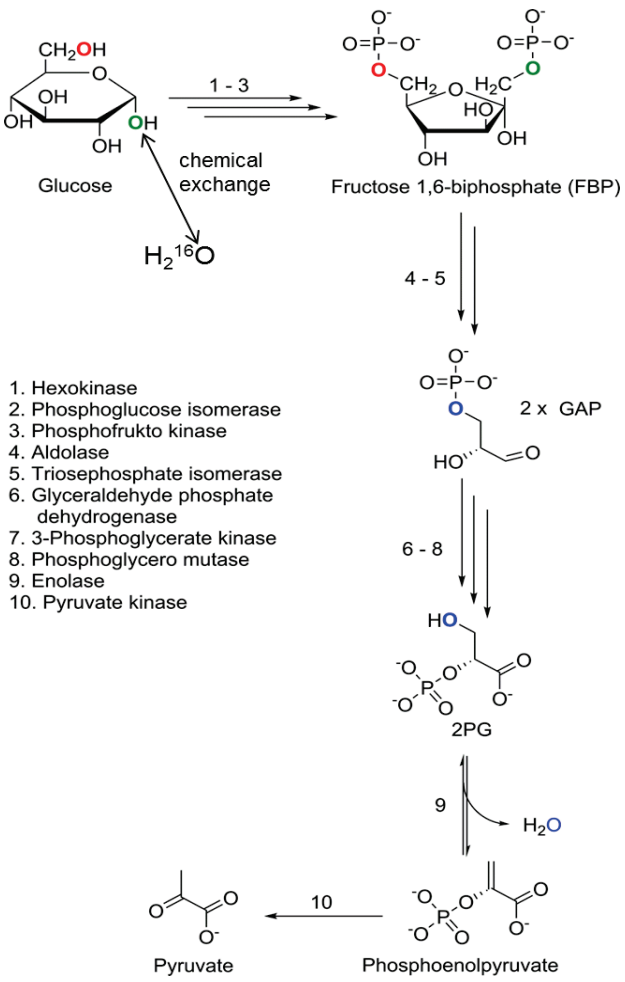

Figure 1: Degradation of ^{17}O-labeled glucose at the C-1 (green) and C-6 positions (red) via glycolysis in ten steps to the final product pyruvate is shown. Chemical exchange of the C1-OH label with water in blood can take place before glycolysis. In the end of the TIM reaction two ^{17}O-labeled GAP molecules (blue) are formed from one FPB molecule. Note that both glucose isotopologues (Glc-1 and Glc-6) lead to a labeled and an unlabeled GAP. Furthermore, each GAP is converted into 2-phosphoglycerate (2PG). Finally, $H_2{}^{17}O$ is cleaved off from each 2PG molecule by the enzyme enolase to form phosphoenolpyruvate (PEP).

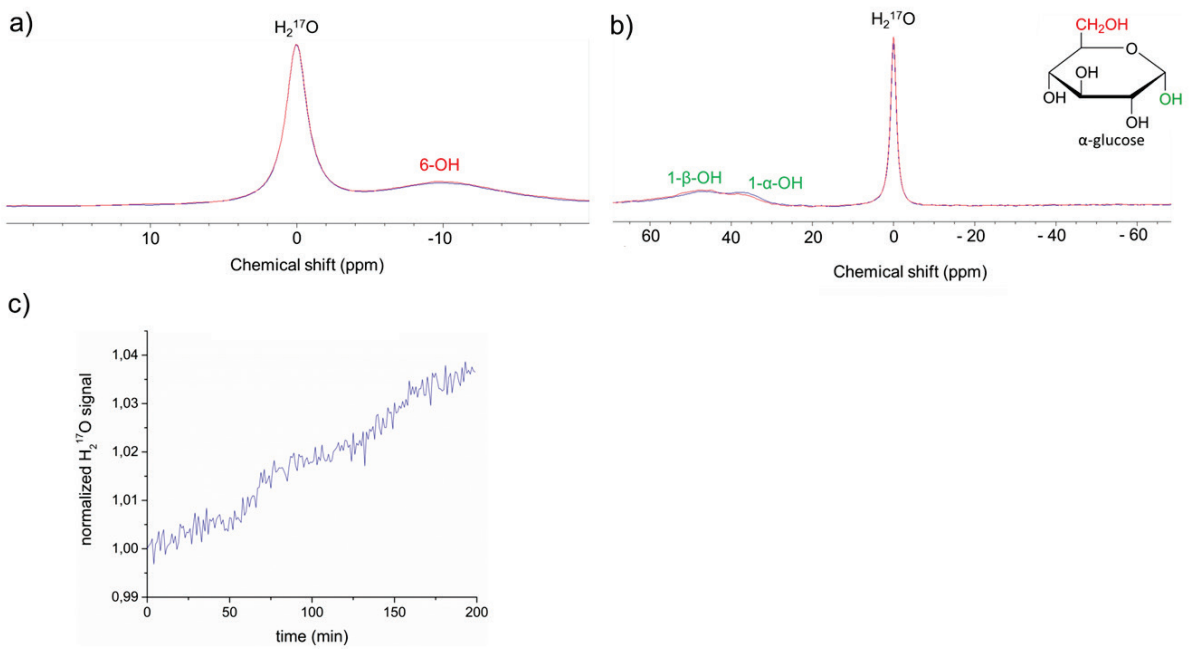

Figure 2: Two representative ^{17}O MRS (f_0 = 67.8 MHz) spectra are shown from the start (t_{start} = 0 min, blue) and end (t_{end} = 200 min, red) of the **(a)** Glc-6 **(b)** Glc-1 chemical exchange experiment performed with a temporal resolution of 1 min. The α (36 ± 1 ppm) and β (47 ± 1 ppm) forms of the anomeric hydroxyl oxygen can be detected at physiological temperature (37°C). **c)** Normalized signal dynamics (peak height) of the $H_2{}^{17}O$ (set to 0 ppm, line width FWHM =1 ppm) resonance are shown over the time course of 200 min.

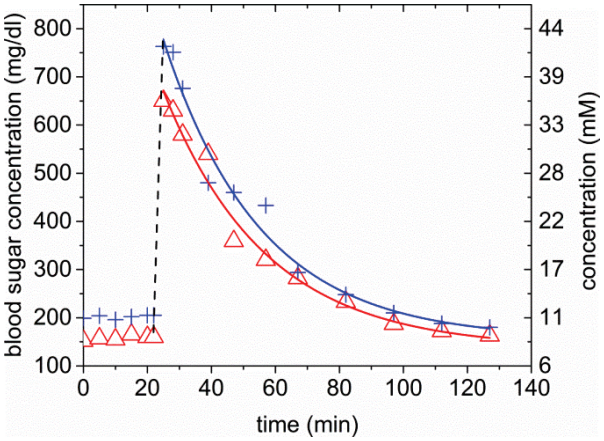

Figure 3: Time courses of two venous blood glucose concentration experiments (red, blue) after administration of 80 mg of unlabeled glucose in 200 µl (0.9 % NaCl) and fits (solid line) with an exponential decay. In both blood sugar measurements the glucose level increases instantaneously to its maximum 42/ 36 mM value and then returns exponentially to the mean baseline concentration of 11/ 9 mM. Increase of glucose concentration level from baseline is indicated as a dashed line.

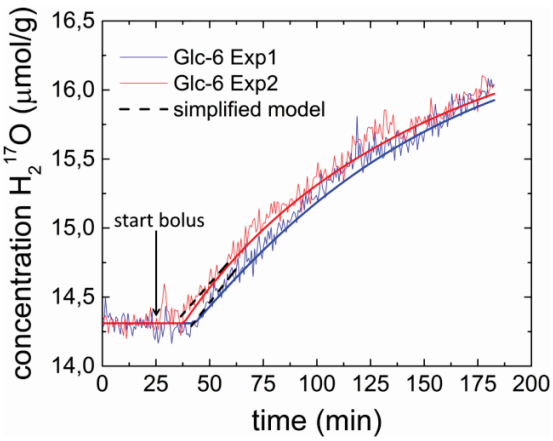

Figure 4: Two representative $H_2^{17}O$ concentration time-courses for the Glc-6 experiments Exp1 and Exp2 and pharmacokinetic model fits in red respectively blue and simplified model fits are shown. Glucose bolus (80 mg Glc-6 dissolved in 200 µl 0.9 % NaCl) was given at t = 27 min. Note that presented data was acquired using the same experimental parameters and setup as described in [2]. Both concentration-time curves show very similar dynamics and initial slopes.

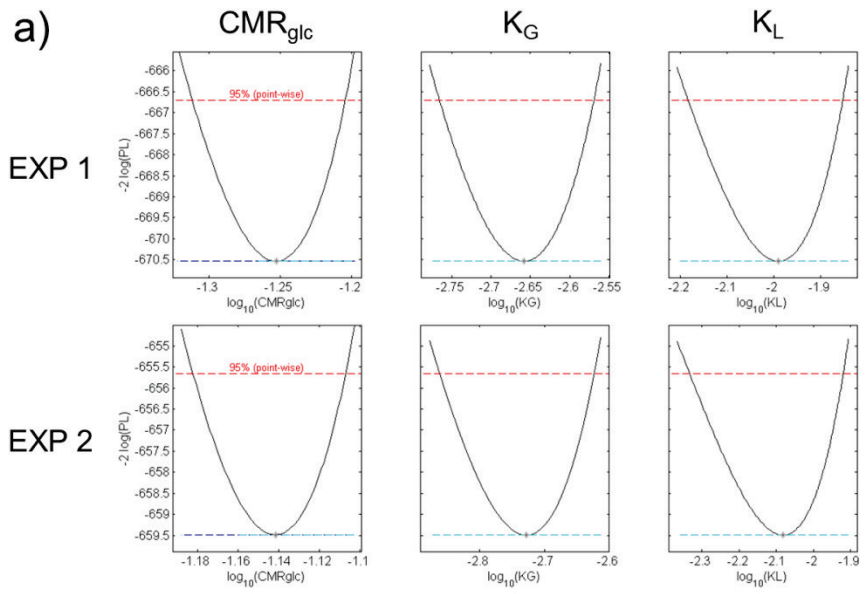

b)

Exp	CMR_{glc}	K_G	K_L
1	0.05-0.06	0.002-0.003	0.007-0.010
2	0.07-0.08	0.001-0.002	0.005-0.010

Figure 5: **a)** Profile likelihood analysis of the parameters $CMR_{Glc,}$ K_L and K_G of the pharmacokinetic model. Confidence intervals are indicated by the red dashed lines. **b)** The identifiability of the rates $CMR_{Glc,}$ K_L and K_G is proved by finite confidence intervals. The rates $CMR_{Glc,}$ K_L and K_G have units of µmol/g/min.

The first observation of ^{17}O MRI in normal rats at 21.1 T

Victor D. Schepkin[1], Andreas Neubauer[2], Christian Schuch[3], Tilo Glaeser[3], Michael Kievel[3], Steven L. Ranner[1], William W. Brey[1], Shannon Helsper[1], and Lothar Schad[2]

[1]CIMAR, NHMFL/FSU, Tallahassee, FL, United States, [2]University of Heidelberg, Mannheim, Germany, [3]NUKEM Isotopes, Alzenau, Germany

SYNOPSIS The capability of ^{17}O MRI in a rat head was evaluated at the high magnetic field of 21.1 T (NHMFL, Tallahassee). The results demonstrated that ^{17}O MR relaxation times are dependent on the magnetic field strength which correlates with experimental observations for sodium. Well separated MR peaks of ^{17}O water and 6-^{17}O glucose provided the time courses of water distribution and glucose consumption in vivo. 3D ^{17}O MRI is possible with a resolution of 1 mm^3 in normal rats. ^{17}O MRI is a promising tool for future tumor detection and evaluation of tumor glucose consumption rates.

INTRODUCTION The natural abundance ^{17}O MR signal in vivo ranks third after proton and sodium. For the same acquisition interval, the ^{17}O signal is 3 times less than sodium [1]. Thus, the capability of the ^{17}O MRI for in vivo studies at the magnetic field of 21.1 T (NHMFL, Tallahassee) is a promising tool. It is already expected that the increased magnetic field can bring a gain in scan time or in imaging resolution. However, the ultra-high magnetic field can also change ^{17}O MR relaxation times, which will be demonstrated below. The main goal of this study is to explore the capability of ^{17}O in vivo MRI at 21.1 T and present the results of using labeled ^{17}O glucose and ^{17}O water as the first steps for future tumor detection based on the Warburg effect.

METHODS The MR experiments were performed on a 21.1 T magnet using Bruker MRI Avance III console (PV 5.1). The MR frequency for ^{17}O was 121.65 MHz. The in vivo RF probe has a double tuned $^{17}O/^{1}H$ *volume* RF coil with an internal diameter of 33 mm, covering the whole rat head. Duration of the 90 RF pulse for ^{17}O in vivo was 165 µs. The ^{17}O MR relaxation times T_1 and T_2 were measured using 180°-t-90° or 90°-t-180° pulse sequences respectively using 256 steps, NA = 16. Both data were fitted by a single exponential function. 3D MR rat head imaging scans were performed using a modified Bruker UTE pulse sequence with voxel of 1 mL, matrix 64x64x64, FOV=64x64x64 mm, TR = 15 ms, TE = 0.2 ms, NA = 16 for natural ^{17}O abundance or NA=1 after ^{17}O enrichments. Scan time in the last case was 1.5 min. The time course of ^{17}O MR signal was investigated after IV tail injections of 1 mL PBS solution containing 17% enriched $H_2{}^{17}O$ or 1.5 ml of PBS with 500 mg of 6-^{17}O 47% enriched D-glucose. The in vivo experiments were performed using 3 male Fisher 344 rats (~ 200 g). All animal experiments were conducted according to the protocols approved by The Florida State University ACUC.

RESULTS AND DISCUSSION The relaxation times T_1 and T_2 at 21.1 T are presented in comparison to the previous data of others at a lower magnetic field [2, 3] (Fig. 1). It was found that T_2 of ^{17}O in a rat head was 2.07 ± 0.03 ms (n = 3), which is much less than the 3.03 ms found earlier at 9.4 T [2]. The corresponding T_1 relaxation time at 21.1 T was 5.35 ± 0.09 ms (n=3), which is a bit higher than at 9.4 T and close to 16.4 T [3]. Additionally, the ^{17}O MR relaxation times in 0.45% saline solution, are both larger at 21.1 T (T_1 = 7.6 ± 0.24 ms, T_2 = 6.5 ± 0.2 ms) than at 9.4 T (T_1= 6.5 ms, T_2=4.1 ms) [2]. Thus, the ^{17}O MR relaxation mechanism is dependent on the strength of the magnetic field, as was also observed for sodium [4, 5]. 3D MRI of ^{17}O in a rat head can be acquired with a resolution of 1x1x1 mm with a scan time of 1.5 min after an IV injection of 1 ml of 17% enriched $H_2{}^{17}O$ (Fig. 2). The image acquired one minute after ^{17}O water injection demonstrated the increased perfusion of the rat brain and cortical areas. The ^{17}O water signal decreased after the injection due to its distribution inside the rat body with the exponential decay time of 11 ± 0.4min (n=2). Injection of the 6-^{17}O labeled glucose yielded in 1.5 minutes a separate MR peak of glucose well separated from the ^{17}O water signal (Fig. 3). The glucose peak, after the initial bolus passage, was slowly decreasing as a result of glucose metabolism (Fig 3). The exponential

glucose breakdown time was 48.2 ± 1.9 min (n=2). At the same time the rate of increase for the ^{17}O MR water peak was ~ 1.5 times less.

CONCLUSION The results demonstrate that ^{17}O MR relaxation times are dependent on the strength of the magnetic field which correlates with the earlier observations for sodium. The well separated ^{17}O MR signals of glucose and water at the ultra-high magnetic field and the corresponding time courses provided separate rates of water distribution and glucose consumption in the rat head. 3D ^{17}O MRI is possible with a resolution of 1 mm^3 in the rat head. Thus, enriched oxygen MRI can be a promising tool for future tumor detection based on the Warburg hypothesis and for evaluating the rates of glucose metabolism in tumors.

ACKNOWLEDGEMENTS The study was performed at the National High Magnetic Field Laboratory (Tallahassee) supported by NSF, grant No. DMR-115490. Many thanks to Richard Desilets, Ashley Blue, Jason Kitchen, Malathy Elumalai, and Peter Gor'kov for their valuable help with RF probes.

References

[1] Budinger T, Bird M, Frydman L, et al. Towards 20 T magnetic resonance for human brain studies: opportunities for discovery and neuroscience rationale. MAGMA, Magnetic Resonance Materials in Physics, Biology and Medicine (Magn Reson Mater Phy) 2016; 1-23. [2] Zhu X, Merkle H, Kwang J, et al. ^{17}O relaxation time and NMR sensitivity of cerebral water and their field dependence. Magn Reson Med. 2001; 45:543-549. [3] Lu M, Zhang Y, Ugurbil K, et al. In vitro and in vivo studies of ^{17}O NMR sensitivity at 9.4 and 16.4 T. Magn Reson Med. 2013; 69:1523-1527. [4] Schepkin V. Sodium MRI of glioma in animal models at ultrahigh magnetic fields. NMR Biomed. 2016; 29:175-186. [5] Nagel A, Umathum R, Rosle M, et al. ^{19}K and ^{23}Na relaxation times and MRI of rat head at 21.1 T. NMR in Biomed. 2016; 29:759-766.

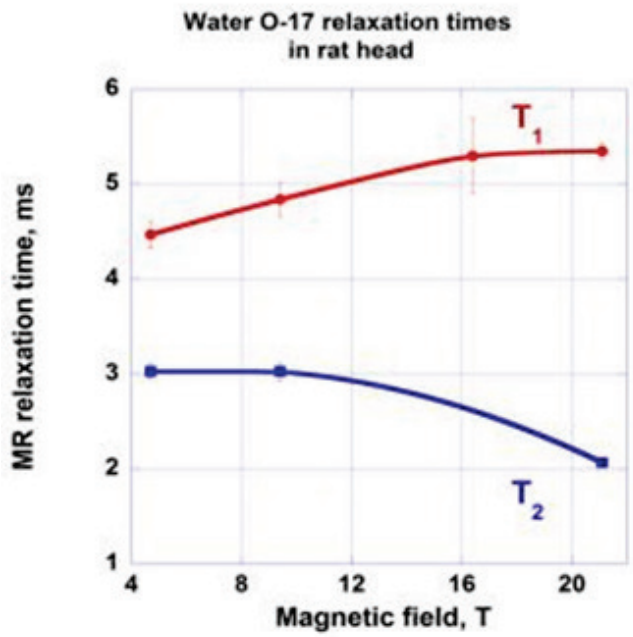

Fig. 1.: Magnetic field strength dependence of ^{17}O MR relaxation times in a rat head. The data at 21.1 T is presented relative to the lower field data of others 2, 3. Note the decrease of the T2 relaxation time at the high magnetic field.

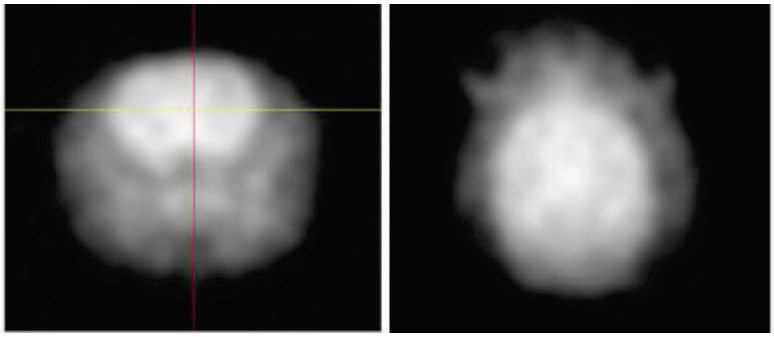

Fig. 2.: ^{17}O 3D MRI of rat head 1 min after injection of 17% enriched $H_2{}^{17}O$. Scan time was 1.5 min, resolution 1x1x1 mm. Note the increased perfusion in all areas of the rat brain and in the cortical areas.

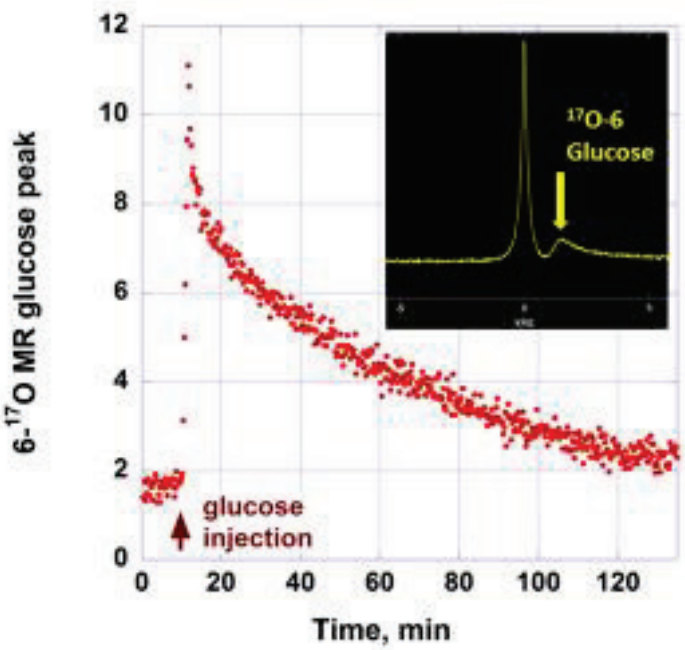

Fig. 3.: The time course of metabolic ^{17}O MR glucose signal decrease in a rat head after IV injection of the ^{17}O labeled glucose. Each point represents a 6-^{17}O glucose MR peak with a step of 15 s. The insert demonstrates one of such peaks, when the glucose MR signal is maximum. The MR peak of 6-^{17}O glucose is at -12.3 ppm relative to ^{17}O water peak. Glucose signal in the rat head after the initial quick bolus passage was fitted reasonably well by the exponential function with a decay time of 48.2 ± 1.9 min (n=2).

Oxygen-17 in the form of water

Oxygen-17 in the form of water is the perfect precursor for the synthesis of NMR active molecules.

As a novel development we recently synthesized ^{17}O labeled D-glucose from our ^{17}O-enriched water. After successful application of the ^{17}O labeled glucose (see above abstracts), we are now convinced that there are several other molecules which can be synthesised from ^{17}O enriched water and can be used for studying Oxygen metabolic pathways by magnetic resonance technology.

In the following you can find an ISMRM abstract, providing you with additional information about our booth wall (ISMRM 2017) (p.16-17). Furthermore, we included a MR-Bibliography about earlier ISMRM abstracts and publications about Oxygen-17.

Enrichment	^{17}O > 10at% - 90at%
Purity	> 99.9%
Volumes	Available in various volumes. Please contact us.
pH	6 - 8

Al	≤ 0,05* ppm
Br	≤ 0,5* ppm
Ca	≤ 0,1* ppm
Cl	≤ 0,5* ppm
Co, Cr, Cu	≤ 0,01* ppm
F	≤ 0,05* ppm
Fe	≤ 0,01* ppm
K	≤ 0,1* ppm

Mg	≤ 0,05* ppm
Mn	≤ 0,01* ppm
Na	≤ 1* ppm
Ni	≤ 0,01* ppm
NO_2	≤ 0,1* ppm
NO_3	≤ 0,05* ppm
Si	≤ 1* ppm
SO_4	≤ 0,1* ppm
Pb	≤ 0,01* ppm
PO_4	≤ 0,05* ppm
Zn	≤ 0,05* ppm

* applicable for 10at% enriched and 20at% enriched ^{17}O water only!

Our Oxygen-17 products are manufactured in accordance with cGMP regulations and with the requirements of 21 Code of Federal Regulations: PARTS 210 and 211.

Information about our ISMRM booth wall

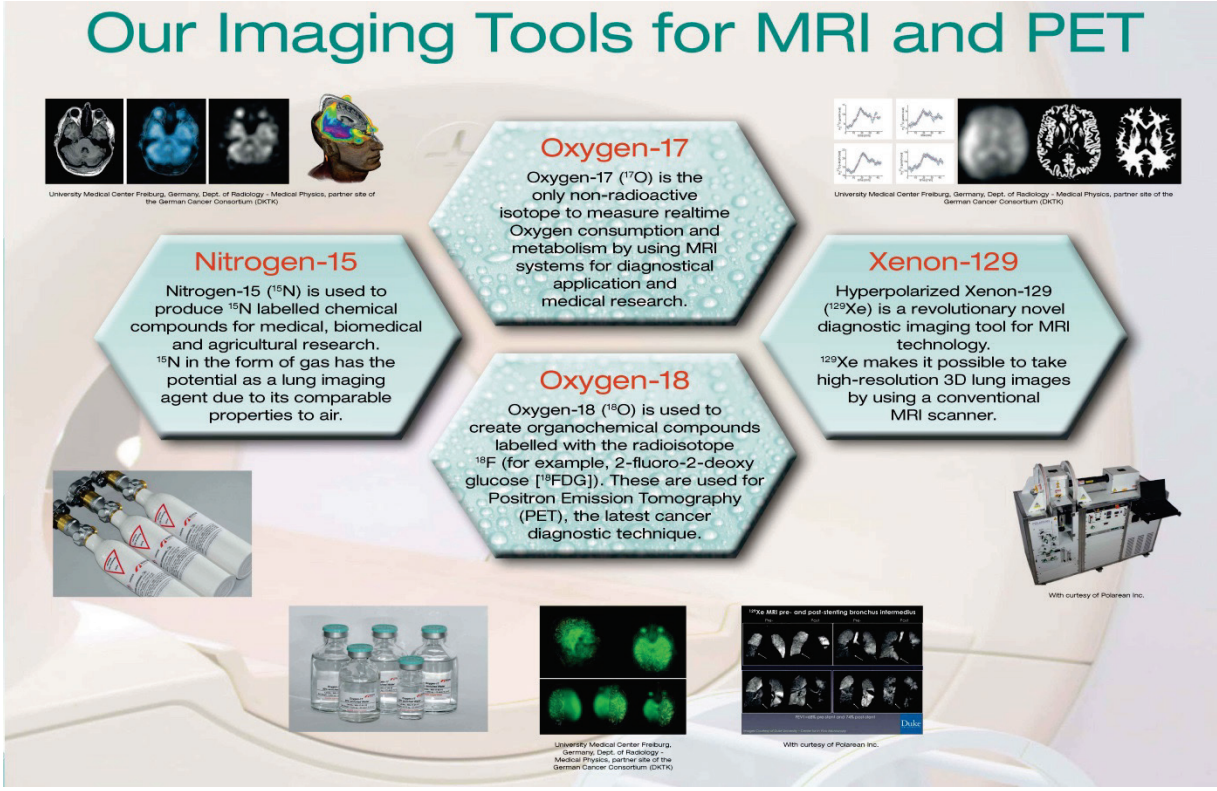

ISMRM-Abstract (booth wall information)

Dynamic ^{17}O-MRI at 3 Tesla for in vivo $CMRO_2$ Quantification

Robert Borowiak[1,2], Dmitry Kurzhunov[2], Philipp Wagner[2], Marco Reisert[2], and Michael Bock[2]

[1]German Cancer Consortium (DKTK), German Cancer Research Center (DKFZ), Heidelberg, Germany, [2]Dept. of Radiology · Medical Physics, University Medical Center Freiburg, Freiburg, Baden-Württemberg, Germany

Introduction Malignant tumors predominately gain energy by high aerobic glycolysis (Warburg effect [1]). The metabolism of tumor cells in the brain can be monitored by assessing their cerebral metabolic rate of oxygen consumption ($CMRO_2$). Clinically, $CMRO_2$ is quantified with positron emission tomography (PET) using radioactively-labelled ^{15}O. Unfortunately, ^{15}O-PET is difficult to perform, because the procedure exposes the patient to ionizing radiation, and the short half-life of ^{15}O (about 2 ms) requires onsite isotope production with a cyclotron. Another possibility to quantify CMRO2 is direct ^{17}O-MRI at 7 or 9.4 Tesla [2, 3]. Un- fortunately, high field MR systems are limited to a few academic institutions, and are not found in clinical routine. Recently, feasibility of cerebral and cardiac ^{17}O-MRI has been demonstrated at natural abundance at clinical field strength of 3 Tesla [4, 5]. In this work we show for the first time direct cerebral dynamic ^{17}O-MRI in a volunteers head at a field strength of 3 Tesla, which is commonly available in a clinical routine.

Materials and Methods The ^{17}O-MRI measurements were performed at a clinical 3 Tesla MR system (Tim Trio, Siemens) using a custom-built Tx/Rx ^{17}O head coil [5] tuned to the ^{17}O resonance at f_0 = 16.7 MHz. For efficient administration of 70%-enriched ^{17}O gas (NUKEM Isotopes GmbH, Germany) an MR-compatible re-breathing system was constructed consisting of a re-breathing mask and a demand oxygen delivery system (DODS, Oxytron3 Weinmann Hamburg, Germany) for gas supply. To demonstrate reproducibility of the gas

administration and to optimize the spatial resolution, two ^{17}O inhalation experiments were performed in a healthy volunteer (male, age 49y) with a nominal isotropic resolution of 10 and 8 mm. In the experiments ^{17}O MR images were acquired during a baseline phase of 10 min under free breathing, an inhalation DODS- phase (4-5 min) when ^{17}O was administered, a re-breathing phase (5-8 min) with a closed rebreathing circuit, and a final wash-out phase (22-25 min), during which the volunteer was breathing room air. In total, 2.7 and 2.5 liter of enriched ^{17}O gas were delivered during the two measurements.

A complete ^{17}O measurement consisted of 45 3D data sets of the brain with a tempo- ral resolution of 1 min using an implemented density-adapted projection sequence (DAPR) [6]. Each data set in experiment 1/ 2 was acquired with the following imaging parameters: nominal resolution (10/ 8 mm)^3, TE = 0.52 ms, TR = 8/ 7 ms, Tpulse = 0.8 ms, BW = 150/ 175 Hz/px, TRO = 6.7/ 5.7 ms, α = 69°, 1 average, 7500/ 8570 projections x 128 sample points per projection interpolated onto a 128³ matrix. The ^{17}O data were reconstructed based on Kaiser-Bessel regridding algorithm without using any filter (e.g. Hann window) [7]. To improve the SNR, view sharing was performed by adding 3 consecutive k-space data sets. Additionally, for co-registration and segmentation of brain compartments 1H data were acquired (Fig.1) using a 3D MPRAGE sequence with the following parameters: TE = 2.86 ms, TR = 2300 ms, TI = 1100 ms, BW = 130 Hz/px, α = 12°, 1 average, FOV = (262 x 300) mm^2, SL = 1 mm, nominal resolution (0.6 x 0.6 x 1) mm^3, matrix: 448 x 512, TAQ = 8:36 min. To obtain $CMRO_2$ values, gray matter (GM) and white matter (WM) regions were segmented, and a 4-phase model [3] was fitted to the signal-time curves using a non-linear least squares method (Fig. 2).

RESULTS AND DISCUSSION In both experiments an increase during and after ^{17}O administration of 20-24 % was seen both in GM and in WM. The $CMRO_2$ values for GM and WM are in a good agreement with literature values for 10 mm voxel size (Fig. 3), whereas the values for higher spatial resolution of 8 mm exceed literature values by 27-65%. In the 10 mm data sets an SNR of 12 was seen, and at 8 mm a lower SNR of 7 was observed, which might account for inaccuracies during $CMRO_2$ quantification due to the non-linear behavior of the magnitude signal at low SNR [9]. To overcome this limitation at higher spatial resolution, ^1H-constraint reconstruction could be applied.

In conclusion, two experiments were successfully performed at clinical field strength of 3 Tesla using a dedicated breathing system. These experiments are a first step to apply direct ^{17}O-MRI in tumor patients to investigate the oxygen turnover in oncology.

Proc. Intl. Soc. Mag. Reson. Med. 23 (2015) 4633.

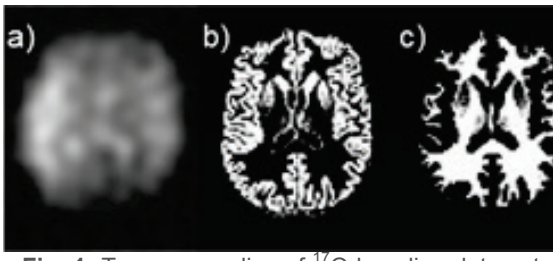

Fig. 1: Transverse slice of ^{17}O baseline data set (10 min) with 10 mm nominal resolution and SNR = 25; and segmented gray (b) and white matter (c) compartments used for $CMRO_2$

Tissue	$CMRO_2$ [µmol/g_{tissue}*min] 3 T, 10 mm	3 T, 8 mm	7 T, 9.4 mm	PET
Gray Matter	1.59±0.16	2.02±0.28	1.65±0.29	1.59±0.23
White Matter	0.71±0.07	1.07±0.15	0.83±0.14	0.65±0.10

Fig. 3: $CMRO_2$ values obtained with direct ^{17}O-MRI at 3 Tesla compared with literature values from 7 Tesla [3] and PET [8].

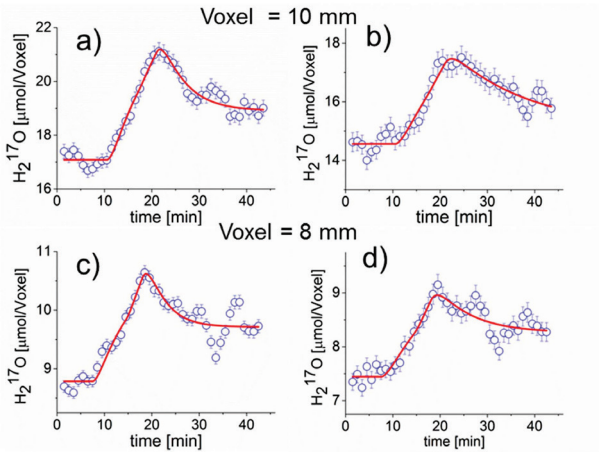

Fig. 2: Signal time courses for voxel sizes of 10 and 8 mm in gray (a, c) and white matter (b, d) are shown in absolute units of H_2 ^{17}O [µ mol/voxel] and fitted with a four phase metabolic model

Oxygen-17 Bibliography

ISMRM 2016 Abstracts/Presentations

1. Dmitry Kurzhunov, Robert Borowiak, Marco Reisert, Philipp Wagner, Axel Krafft, and Michael Bock; 3D $CMRO_2$ mapping in human brain with direct ^{17}O-MRI and proton-constrained iterative reconstructions; Program Number 1470
2. Hannes Michel Wiesner, Xiao-Hong Zhu, Kamil Ugurbil, and Wei Chen; Sensitivity Comparison of Ultrahigh-field Oxygen-17 MRS Imaging between 7T and 10.5T using a Human Head Size Phantom and Quadrature Surface Coil; Program Number: 3942
3. Ruomin Hu, Andreas Neubauer, Jorge Chacón-Caldera, Javier Uranga Solchaga, Christian Schuch, Tilo Gläser, Cordula Nies, Eric Gottwald, Stefan Giselbrecht, and Lothar R. Schad; In Vitro Oxygen-17 NMR Spectroscopy of Cellular Metabolism at Ultra High Field; Program Number 3963
4. Robert Borowiak, Wilfried Reichardt, Dmitry Kurzhunov, Christian Schuch, Jochen Leupold, Thomas Lange, Marco Reisert, Axel Krafft, Elmar Fischer, and Michael Bock; Initial investigation of glucose metabolism in mouse brain using enriched 17O-glucose and dynamic 17O-MRS; Program Number 3964
5. Sebastian C. Niesporek, Reiner Umathum, Thomas M. Fiedler, and Armin M. Nagel; Evaluation of High Temporal and Spatial Resolution ^{17}O-MRI; Program Number 3965
6. Sebastian C. Niesporek, Reiner Umathum, Thomas M. Fiedler, and Armin M. Nagel; Iterative Approach for Partial Volume Corrected T2* Determination in 17O-MRI; Program Number 3966

ISMRM 2015 Abstracts/Presentations

1. Borowiak, R., Kurzhunov, D., Wagner, P., Reisert, M., Bock; Dynamic ^{17}O-MRI at 3 Tesla for In Vivo $CMRO_2$ Quantification; Program Number: 4633
2. Zhang, Y., Erokwu, B. O., Liu, Y., Farr, G. W., Boron, W. F., Flask, C. A., Yu, X.; Assessing Water Influx and Retention in the Brain of AQP4 Knockout Mice by ^{17}O-MRI; Program Number: 1997.
3. Najac, C., Tiret, B., Flament, J., Guillermier, M., Houitte, D., Badin, R.A., Hantraye, P., Brouillet, E., Lebon, V., Valette, J., $CMRO_2$ Quantification by Direct ^{17}O MRI at 7 T in the Macaque Brain: Assessment of Energy Metabolism Impairment In Vivo; Program Number: 4615.
4. Zhu, X-H., Wiesner, H. M., Lee, B-Y., Lu, M., Ugurbil, K., Chen, W.; Quantitative and Simultaneous Imaging of $CMRO_2$, CBF and OEF in Resting Human Brain; Program Number: 0895.

ISMRM 2014 Abstracts/Presentations

1. Borowiak, R., Groebner, J., Kurzhunov, D., Fischer, E., Dragonu, I., Bock, M.; Direct Cerebral ^{17}O-MRI at a Clinical Field Strenght of 3 Tesla Using a Tx/Rx Head Coil; Program Number: 0687.
2. Zhu, X-H., Liu, X., Lu, M., Wiesner, H M., Ugurbil, K., Chen, W,; In Vivo ^{17}O MR Imaging and Quantification of $CMRO_2$, CBF and OEF in Human Visual Cortex at Rest and During Activation; Program Number: 3763.
3. Augath, M A., Seuwen, A., Zwick, S., Rudin, M.; Increase in Sensitivity and Signal Stability in ^{17}O MRI Using a Cryogenic RF Probe; Program Number: 2972.
4. Möllenhoff, K., Felder, J., Romanzetti, S., Gordji-Nejad, A., Shah, N J., Natural Abundance in Vivo ^{17}O Measurements at 9.4T; Program Number: 0475.
5. Barbier, E., Mapping Blood Flow & Tissue Oxygenation with MRI: Insights from Other Modalities
6. Cerdán, S.; Subject: Bamboc; MR Spectroscopy: The Promise; Program Number: 1027.

ISMRM 2013 Abstracts/Presentations

1. Romanzetti, S., Fiege, D. P., Shah, N.J., 3D TWIRL: A Novel K-Space Trajectory for Imaging of Fast Relaxing Nuclei; Program Number: 3965.
2. Hoffmann, S. H., Meise, F. M., Biller, A., Nagel, A. M.; Adaptive Combination of Multichannel Data for Non-Proton MRI; Program Number: 1983.
3. Groebner, J., Borowiak, R., Rösler, M., Umathum, R., Fischer, E., Pavlina, J. M., Bock, M.; In Vivo ^{17}O-MRI at 3 Tesla Using a TxRx Surface Coil; Program Number: 1985.
4. Lee, J.-H., Norris, M., Fugate, E. M., Avdievich, G. I., Hetherington, H. P.; A Novel Double Tuned 4T ^{1}H/^{17}O Head Volume Coil; Program Number: 2784.
5. Cui, W., Zhu, X.-H., Vollmers, M., Colonna, E., Adriany, G., Tramm, B., Dubinsky, J., Oz, G., Oxygen-17 MRS for $CMRO_2$ Measurements in the Mouse Brain at 16.4T; Program Number: 0863.
6. Hoffmann, S. H., Radbruch, A., Semmler, W., Nagel, A. M.; . Partial Volume Corrected $CMRO_2$ Determination in a Glioblastoma Patient by ^{17}O MRI; Program Number: 0216.

7. Wang, X., Zhu, X.-H., Zhang, Y., Chen, W., Significant BOLD Signal Reduction Induced by Perfluorocarbon Emulsion in the Rat Brain; Program Number: 0848.
8. Boros, E., Polasek, M.v., Zhang, Z., Caravan, P.A.; Single Amino Acid Gd-Complex as a Modular Tool for High Relaxivity MR Contrast Agent Development; Program Number: 1900.
9. Atkinson, I. C., Ultra-High Field MR: Multi-Nuclear Imaging, Symposium - Emerging Technologies for Clinical Neuroimaging; Program Number: 007006

ISMRM 2012 Abstracts/Presentations

1. Pilkinton, D. T., Babu, V. K., Baker, W., Greenberg, J. H., Reddy, R., Hyperoxic Calibrated Quantitative fMRI for the Measurement of Regional Cerebral Metabolic Rate of Oxygen in a Hypermetabolic Swine Model; *Program; Proc. Intl. Soc. Mag. Reson. Med. 20 (2012)*; Number: 2912
2. Zhu, X.-H., Chen, W., In Vivo ^{17}O Measurements of Water Rotational Correlation Time and Hydrodynamic Radius in Rat Brain; *Proc. Intl. Soc. Mag. Reson. Med. 20 (2012);* Program Number: 1821
3. Wiener, E. C., Sengar, R., Elst, L. V., Abadjian, M.-C., Moore, C.E., Rheingold, A. L., Grotjahn, D., New Bifunctional Chelates with Optimal Water Residence Times for Molecular Imaging; *Proc. Intl. Soc. Mag. Reson. Med. 20 (2012)*; Program Number: 0793
4. Zheng, J., Muccigrosso, D., Bashir, A., Gupte, P., Gropler, R. J.; Quantitative Cardiac ^{17}O MRI: Initial Validation Study; *Proc. Intl. Soc. Mag. Reson. Med. 20 (2012)*; Program Number: 3887.
5. Liu, P., Xu, F., Lu, H.; A Turn-Key Solution for the Quantification of Brain Oxygen Metabolism; *Proc. Intl. Soc. Mag. Reson. Med. 20 (2012);* Program Number: 471.

ISMRM 2011 Abstracts/Presentations

1. Atthe B, Kemerer M, Chen Y, et al. Quantitative Assessment of Mitochondrial Metabolic Efficiency by ^{17}O and ^{31}P MR Spectroscopy in Isolated Rat Hearts. *Proc. Intl. Soc. Mag. Reson. Med. 19 (2011).*
2. Muccigrosso D, He X, Abendschein D, et al. Methods for Quantification of Absolute Myocardial Oxygen Con- sumption with ^{17}O-CMR. *Proc. Intl. Soc. Mag. Reson. Med. 19 (2011)*.
3. Meise FM, Groebner J, Nagel AM, et al. A 30-Channel Phased Array for Oxygen-17 (^{17}O) Brain MRI at 7 Tesla. *Proc. Intl. Soc. Mag. Reson. Med. 19 (2011)*.
4. Hoffmann SH, Nagel AM, Meise FM, Umathum R, Bock M. In Vivo Relaxation Parameters of Oxygen-17 (^{17}O). Proc. Intl. Soc. Mag. Reson. Med. 19 (2011).
5. Zhu X-H, Chen J, Tu T-W, Chen W, Song S-K. Exploring the New Utility of the ^{17}O-MRS Imaging Technique for Studying CMRO2 and Perfusion in Stroke Mice. *Proc. Intl. Soc. Mag. Reson. Med. 19 (2011).*
6. Wiesner HM, Pohmann R, Balla DZ, Chen W, Ugurbil K, Uludag K. Measurement of CMRO2 Changes by Soma- tosensory Stimulation in Rat Using Oxygen-17 at 16.4T. *Proc. Intl. Soc. Mag. Reson. Med. 19 (2011).*
7. Kassey VB, Baker W, Mesquita RC, et al. Preliminary Studies to Assess $CMRO_2$ with Integrated T1 Rho MRI and Hybrid DRS/DCS Optical Approach in Clinical Scanners. *Proc. Intl. Soc. Mag. Reson. Med. 19 (2011).*
8. Mateescu GD, Flask CA, Duerk JL. Novel Approach for the Assessment of the Bioavailability of Exogenous Phos- phate by in Vivo Dynamic ^{17}O and ^{31}P MRS and MRI. *Proc. Intl. Soc. Mag. Reson. Med. 19 (2011).*
9. Lu M, Wang X, Taylor R, et al. In Vitro and In Vivo Studies of ^{17}O NMR Sensitivity at 9.4 and 16.4 Tesla. *Proc. Intl. Soc. Mag. Reson. Med. 19 (2011).*
10. Kirsch S, Schad LR. Single-Slice Mapping of Submillisecond T2 Using Spin Echo Prepared Ultra-Short Echo Time Imaging. *Proc. Intl. Soc. Mag. Reson. Med. 19 (2011).*

ISMRM 2010 Abstracts/Presentations

1. Zhu X-H, Zhang Y, Chen W. In Vivo ^{17}O MRS Imaging for Assessing Myocardial Oxygen Metabolism in Rat Heart at 9.4T. *Proc. Intl. Soc. Mag. Reson. Med. 18 (2010).*
2. Zhu X-H, Zhang Y, Wiesner H, Ugurbil K, Chen W. Estimation of CBF Based on the Metabolic $H_2{}^{17}O$ Decay Rate in $CMRO_2$ Measurement Using In Vivo ^{17}O MR Approach. *Proc. Intl. Soc. Mag. Reson. Med. 18 (2010).*
3. Hoffman S, Begovatz P, Nagel A, Umathum R, Bock M. In Vivo Oxygen-17 (^{17}O) MRI at 7 Tesla. *Proc. Intl. Soc. Mag. Reson. Med. 18 (2010).*
4. Wey H-Y, Du F, Lin A-L, et al. Indirect ^{17}O MRI Using T1ρ at 11.7 T. *Proc. Intl. Soc. Mag. Reson. Med. 18 (2010).*
5. Narazaki M, Kanazawa Y, Ikehira H, Matsuda T. The ^{17}O Imaging for Regional Oxygen Consumption Rate in Tumor Bearing Mice at 7T. *Proc. Intl. Soc. Mag. Reson. Med. 18 (2010)*

6. Lu M, Spires J, Mateescu GD, Flask C, Yu X. Exploration of Mitochondrial Respiration in Isolated Hearts: An Ob- servation from Metabolically Produced $H_2{}^{17}O$ Using ^{17}O NMR Spectroscopy. *Proc. Intl. Soc. Mag. Reson. Med. 18 (2010).*
7. Atkinson IC, Sonstegaard R, Bityou L, Pliskin NH, Thulborn KR. Safety of ^{17}O and ^{23}Na MR Imaging of the Hu- man Brain at 9.4 Tesla. *Proc. Intl. Soc. Mag. Reson. Med. 18 (2010).*

ISMRM 2009 Abstracts/Presentations

1. Wiesner HM, Balla DZ, Pohmann R, Chen W, Ugurbil K, Uludag K. ^{17}O T1/T2* Tissue-Relaxation Rates with Anatomical Contrast in the Rat Brain at 16.4 T. *Proc. Intl. Soc. Mag. Reson. Med. 18 (2010).*
2. Zhu X-H, Zhang Y, Ugurbil K, Chen W. Direct and Noninvasive Measurement of Cerebral Metabolic Rate of ATP in Cat Brain and Its Physiological Implications. *Proc. Intl. Soc. Mag. Reson. Med. 18 (2010).*
3. McCommis KS, He X, Abendschein DR, Gupte PM, Gropler RJ, Zheng J. New Methods for the Quantification of Myocardial Oxygen Consumption with ^{17}O MRI. Proc. Intl. Soc. Mag. Reson. Med. 18 (2010).
4. Atkinson IC, Thulborn KR. Non-Invasive, Whole-Brain $CMRO_2$ Mapping of the Human Brain. *Proc. Intl. Soc. Mag. Reson. Med. 18 (2010).*

Reviews

1. Gordji-Nejad A, Mollenhoff K, Oros-Peusquens AM, Pillai DR, Shah NJ Characterizing cerebral oxygen metabolism employing oxygen-17 MRI/MRS at high fields, *Magn Reson Mater Phy 2014; 27:81–93*
2. Zhu XH, Zhang N, Zhang Y, Zhang X, Ugurbil K, Chen W. In vivo ^{17}O NMR approaches for brain study at high field. *NMR Biomed. Apr 2005;18(2):83-103*.
3. Mateescu GD. Functional oxygen-17 magnetic resonance imaging and localized spectroscopy. *Adv Exp Med Biol. 2003;510:213-8.*

Methods

1. Dmitry Kurzhunov, Robert Borowiak, Helge Hass, Philipp Wagner, Axel Joachim Krafft, Jens Timmer, Michael Bock Quantification of Oxygen Metabolic Rates in Human Brain With Dynamic 17 O MRI: Profile Likelihood Analysis; *Magn Reson Med 2016 Nov 1*.
2. Lou S, Lepak VC, Eberly Le, Roth B, Cui W, Zhu XH, Öz G, Dubinsky JM.; Oxygen consumption deficit in Huntington disease mouse brain under metabolic stress.; *Hum Mol Genet. 2016 Jul 1;25(13):2813-2826*
3. Suzuki K, Igarashi H, Huber VJ, Kitaura H, Kwee IL, Nakada T,; Ligand-Based Molecular MRI: O-17 JJVCPE Amyloid Imaging in Transgenic Mice, *J NeuroImaging Epub 23 FEB 2014*
4. Zhu XH, Zhang Y, Wiesner HN, Ugurbil K, Chen W,; In Vivo Measurement of CBF Using ^{17}O NMR Signal of Metabolically Produced $H_2{}^{17}O$ as a Perfusion Tracer,; *Magn Res Medicine 70:309–314 (2013)*
5. Lu M, Zhang Y, Ugurbil K, Chen W, Zhu XH, In Vitro and In Vivo Studies of ^{17}O NMR Sensitivity at 9.4 and 16.4 T,; *Magnetic Resonance in Medicine 69:1523–1527 (2013)*
6. Zhu XH, Chen JM, Tu TW, Chen W, Song SK Simultaneous and noninvasive imaging of cerebral oxygen metabolic

   rate, blood flow and oxygen extraction fraction in stroke mice, NeuroImage 64:437-447 (2013)
7. Hoffmann SH, Begovatz P, Nagel AM, et al.; A measurement setup for direct (17) O MRI at 7 T. *Magn Reson*

   Med. 2011;66(4):1109-15.
8. Hyder F.; Dynamic Brain Imaging Multi-Modal Methods and In Vivo Applications. 2009
9. Zhu XH, Du F, Zhang N, Zhang Y, Lei H, Zhang X, Qiao H, Ugurbil K, Chen W. Advanced In Vivo Heteronuclear MRS Approaches for Studying Brain Bioenergetics Driven by Mitochondria. *Methods Mol Biol. 2009;489:317-57.*
10. Mellon EA, Beesam RS, Kasam M, Baumgardner JE, Borthakur A, Witschey WR Jr, Reddy R. Single shot T1rho magnetic resonance imaging of metabolically generated water in vivo. *Adv Exp Med Biol. 2009;645:279-86.*
11. de Graaf RA, Brown PB, Rothman DL, Behar KL. Natural abundance ^{17}O NMR spectroscopy of rat brain in vivo. J *Magn Reson. 2008;193(1):63-7.*
12. Thelwall PE. Detection of ^{17}O-tagged phosphate by (31)P MRS: a method with potential for in vivo studies of phosphorus metabolism. *Magn Reson Med. 2007;57(6):1168-72.*
13. Zhu XH, Zhang Y, Zhang N, Ugurbil K, Chen W. Noninvasive and three-dimensional imaging of $CMRO_2$ in rats at 9.4 T: reproducibility test and normothermia/hypothermia comparison study. *J Cereb Blood Flow Metab. 2007; 27: 1225 – 1234.*
14. Tailor DR, Baumgardner JE, Regatte RR, Leigh JS, Reddy R.; Proton MRI of metabolically produced $H_2{}^{17}O$ us- ing an efficient $^{17}O_2$ delivery system. *Neuroimage. 2004;22(2):611-618.*

15. Sood R. Off-resonance binomial preparatory pulse technique for high sensitivity MRI of H_2O-17. *Magn Reson Imaging. 2004;22(2):181-195.*
16. Fiat D, Hankiewicz J, Liu S, Trbovic S, Brint S. ^{17}O magnetic resonance imaging of the human brain. *Neurol Res. 2004;26(8):803-808*.
17. Zhang X, Zhu XH, Tian R, Zhang Y, Merkle H, Chen W. Measurement of arterial input function of ^{17}O water tracer in rat carotid artery by using a region-defined (REDE) implanted vascular RF coil. *MAGMA. 2003;16 (2):77-85.*
18. Zhu XH, Merkle H, Kwag JH, Ugurbil K, Chen W. ^{17}O relaxation time and NMR sensitivity of cerebral water and their field dependence. *Magn Reson Med. 2001;45(4):543-9.*
19. Charagundla SR, Duvvuri U, Noyszewski EA, et al. ^{17}O-decoupled (1)H spectroscopy and imaging with a sur- face coil: STEAM decoupling. *J Magn Reson. 2000;143(1):39-44.*
20. Reddy R, Stolpen AH, Charagundla SR, Insko EK, Leigh JS. ^{17}O-decoupled ^{1}H detection using a double-tuned coil. *Magn Reson Imaging. 1996;14(9):1073-1078.*
21. Reddy R, Stolpen AH, Leigh JS. Detection of ^{17}O by proton T1 rho dispersion imaging. *J Magn Reson B.1995;108(3):276-279*
22. Lasker SE. Functional MR imaging of a metabolite of $^{17}O_2$. *Artif Cells Blood Substit Immobil Biotechnol. 1994;22(4):1055-68.*
23. Ronen I, Navon G. A new method for proton detection of $H_2{}^{17}O$ with potential applications for functional MRI. *Magn Reson Med. 1994;32(6):789-793.*
24. Kwong KK, Xiong J, Kuan WP, Cheng HM. Measurement of water movement in the rabbit eye in vivo using H_2 ^{17}O. *Magn Reson Med. 1991;22(2):443-50.*
25. Hopkins AL, Haacke EM, Barr RG, Tkach J. Oxygen-17 contrast agents. Fast imaging techniques. *Invest Radiol.1988;23 Suppl 1:S240-242.*
26. Hopkins AL, Barr RG. Oxygen-17 compounds as potential NMR T2 contrast agents: enrichment effects of $H_2{}^{17}O$ on protein solutions and living tissues. *Magn Reson Med. 1987;4(4):399-403.*
27. Yeung HN, Lent AH. Proton transverse relaxation rate of ^{17}O-enriched water. *Magn Reson Med. 1987;5(1):87*

Brain

1. Hannes M. Wiesner, Dávid Z. Balla, G. Shajan, Klaus Scheffler, Kâmil Uğurbil, Wei Chen, Kâmil Uludağ and Rolf; 17O relaxation times in the rat brain at 16.4 tesla; *Magnetic Resonance in Medicine Vol. 75, 5, 1886–1893, May 2016*
2. DeLaPaz R, Gupte P.; Potential Application of ^{17}O MRI to Human Ischemic Stroke. *Adv Exp Med Biol. 2011;701:22*
3. Mellon EA, Beesam RS, Elliott MA, Reddy R.; Mapping of cerebral oxidative metabolism with MRI. *Proc Natl Acad Sci U S A. 2010;107(26):11787-92*
4. Atkinson IC, Sonstegaard R, Pliskin NH, Thulborn KR. Vital signs and cognitive function are not affected by ^{23}Na and ^{17}O magnetic resonance imaging of the human brain at 9.4 T. *J Magn Reson Imaging. 2010;32(1):82-7*.
5. Atkinson IC, Thulborn KR. Feasibility of mapping the tissue mass corrected bioscale of cerebral metabolic rate of oxygen consumption using 17-oxygen and 23-sodium MR imaging. *Neuromage. 2010;51(2):723-33.*
6. Zhu X-H, Zhang N, Zhang Y, Ugurbil K, Chen W. New insights into central roles of cerebral oxygen metabolism in the resting and stimulus-evoked brain. *J Cereb Blood Flow Metab.2009;29(1):10–8.*
7. Mellon EA, Beesam RS, Baumgardner, Borthakur A, Witschey WR, Reddy R. Estimation of the regional cerebral metabolic rate of oxygen consumption with proton detected ^{17}O MRI during precision $^{17}O_2$ inhalation in swine. *J Neurosci Methods.2009;179(1):29-39.*
8. Mellon EA, Beesam RS, Baumgardner JE, Borthakur A, Witschey WR, Reddy R. Estimation of the regional cere- bral metabolic rate of oxygen consumption with MRI during the first 60 seconds of $^{17}O_2$ inhalation in swine. *Proc. Intl. Soc. Mag. Reson. Med. 16 (2008).*
9. Zhu XH, Zhang Y, Zhang N, Ugurbil K, Chen W., Noninvasive and three-dimensional imaging of CMRO(2) in rats at 9.4 T: reproducibility test and normothermia/hypothermia comparison study. *J. Cereb Blood Flow Metab. 2007;27(6):1225-34*
10. Tailor DR, Roy A, Regatte RR, et al. Indirect ^{17}O-magnetic resonance imaging of cerebral blood flow in the rat. *Magn Reson Med. 2003;49(3):479-487.*
11. DeLaPaz RL, Gupte P, Connolly S, Wu E, Brown T. Oxygen-17 Uptake in Mouse Cerebral Ischemia. *Proc. Intl. Soc. Mag. Reson.Med. 11 (2003).*
12. de Crespigny AJ, D'Arceuil HE, Engelhorn T, Moseley ME. MRI of focal cerebral ischemia using ^{17}O-labeled water. *Magn Reson Med. 2000;43(6):876-883.*
13. Ronen I, Merkle H, Ugurbil K, Navon G. Imaging of $H_2{}^{17}O$ distribution in the brain of a live rat by using proton-detected ^{17}O MRI. *Proc Natl Acad Sci U S A. 1998; 95 (22):12934-12939.*

14. Arai T, Nakao S, Morikawa S, et al. Measurement of local cerebral blood flow by magnetic resonance imaging: in vivo autoradiographic strategy using ^{17}O-labeled water. *Brain Res Bull. 1998;45(5):451-456.*
15. Pekar J, Sinnwell T, Ligeti L, Chesnick AS, Frank JA, McLaughlin AC. Simultaneous measurement of cerebral oxy- gen consumption and blood flow using ^{17}O and ^{19}F magnetic resonance imaging. *J Cereb Blood Flow Metab. 1995;15(2):312-320.*
16. Fiat D, Dolinsek J, Hankiewicz J, Dujovny M, Ausman J. Determination of regional cerebral oxygen consumption in the human: ^{17}O natural abundance cerebral magnetic resonance imaging and spectroscopy in a whole body system. *Neurol Res. 1993;15(4):237-48.*
17. Fiat D, Kang S. Determination of the rate of cerebral oxygen consumption and regional cerebral blood flow by non-invasive ^{17}O in vivo NMR spectroscopy and magnetic resonance imaging. Part 2. Determination of $CMRO_2$ for the rat by ^{17}O NMR, and $CMRO_2$, rCBF and the partition coefficient for the cat by ^{17}O MRI. *Neurol Res. 1993;15(1):7-22*
18. Fiat D, Ligeti L, Lyon RC, et al. In vivo ^{17}O NMR study of rat brain during $^{17}O_2$ inhalation. *Magn Reson Med. 1992;24(2):370-374.*
19. Kwong KK, Hopkins AL, Belliveau JW, et al. Proton NMR imaging of cerebral blood flow using $H_2{}^{17}O$. *MagnReson Med. 1991;22(1):154-158.*
20. Hopkins AL, Lust WD, Haacke EM, Wielopolski P, Barr RG, Bratton CB. The stability of proton T2 effects of oxy- gen-17 water in experimental cerebral ischemia. *Magn Reson Med. 1991;22(1):167-174.*
21. Pekar J, Ligeti L, Ruttner Z, Lyon RC, Sinnwell TM, van Gelderen P, Fiat D, Moonen CT, McLaughlin AC. In vivo measurement of cerebral oxygen consumption and blood flow using ^{17}O magnetic resonance imaging. *Magn Reson Med. 1991;21(2):313-9.*
22. Arai T, Mori K, Nakao S, Watanabe K, Kito K, Aoki M, Mori H, Morikawa S, Inubushi T. In vivo Oxygen-17 nu- clear magnetic resonance for the estimation of cerebral blood flow and oxygen consumption. *Biochem Biophys Res Commun. 1991;179(2):954-61.*
23. Arai T, Nakao S, Mori K, et al. Cerebral oxygen utilization analyzed by the use of Oxygen-17 and its nuclear magnetic resonance. *Biochem Biophys Res Commun. 1990;169(1):153-158.*
24. Hopkins AL, Haacke EM, Tkach J, Barr RG, Bratton CB. Improved sensitivity of proton MR to Oxygen-17 as a contrast agent using fast imaging: detection in brain. *Magn Reson Med. 1988;7(2):222-229.*

Heart & Muscle

1. Borowiak R, Groebner J, Haas M, Hennig J, Bock M, Direct cerebral and cardiac ^{17}O-MRI at 3 Tesla: initial results at natural abundance, *Magn Reson Mater Phy 2014; 27:95–99*
2. Lu M, Atthe B, Mateescub G, Flaska CA, Yua X, Assessing mitochondrial respiration in isolated hearts using ^{17}O MRS NMR *Biomed 2012; 25(6): 883–889*
3. McCommis KS, He X, Abendschein DR, Gupte PM, Gropler RJ, Zheng J. Cardiac ^{17}O MRI: Toward Direct Quan- tification of Myocardial Oxygen Consumption. *Magn Reson Med. 2010;63(6):1442-7.*
4. Rogers WJ, Gupte PM, Piccione EA, Kramer CM, Vido DA, Reichek N. T2 Imaging Using O-17 for Detection of Viability in Myocardial Infarction. *Proc. Intl. Soc. Mag. Reson. Med. 7 (1999).*
5. Fung BM, McGaughy TW. Study of spin-lattice and spin-spin relaxation times of ^{1}H, ^{2}H, and ^{17}O in muscular water. *Biophys J. 1979;28(2):293-303.*
6. Civan MM, Shporer M. Pulsed nuclear magnetic resonance study of ^{17}O, ^{2}D, and ^{1}H of water in frog stri- ated muscle. *Biophys J. 1975;15(4):299-306.*

Oncology

1. Hoffmann SH, Radbruch A, Bock M, Semmler W, Nagel AM, Direct ^{17}O MRI with partial volume correction: first experiences in a glioblastoma patient, *Magn Reson Mater Phy; epub April 1, 2014*
2. Narazaki M, Kanazawa Y, Koike S, Ando K, Ikehira H. Dynamical ^{17}O imaging in tumor bearing mice at 7T. Proc. *Intl. Soc. Mag. Reson. Med. 15 (2007).*
3. Tailor DR, Poptani H, Glickson JD, Leigh JS, Reddy R. High-resolution assessment of blood flow in murine RIF-1 tumors by monitoring uptake of $H_2{}^{17}O$ with proton T(1rho)-weighted imaging. *Magn Reson Med. 2003;49 (1):1-6.*
4. Shporer M, Haas M, Civan MM. Pulsed nuclear magnetic resonance study of ^{17}O from $H_2{}^{17}O$ in rat lymphocytes. *Biophys J. 1976;16(6):601-11.*

Xenon-129 in the form of gas mixtures

Hyperpolarization of Xenon-129 is a revolutionary new diagnostic imaging tool for the magnetic resonance imaging (MRI) technology.

Hyperpolarized Xenon-129 makes it possible capturing high-resolution, 3D images of the lung using a conventional MRI scanner.

Due to the varying solubility of Xenon in different environments, it is additionally possible to illuminate organ functions and tissue characteristics in a total way.

Our cooperation partner Polarean Inc. designs and manufactures equipment for production of hyperpolarized Xenon or Helium gas.

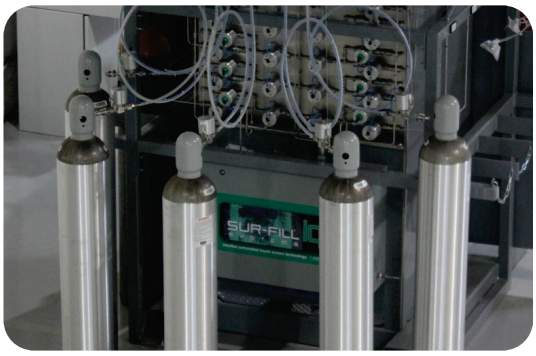

Enrichment	^{129}Xe ≥ 90at% and ^{129}Xe ≥ 80at%
Purity	All mixtures ≥ 99.99%
Volume/Valves	Mixtures: Available in 3,000 liter - 7,000 liter gas cylinder (with CGA 580 valve) Pure Gas: Available in 50 liter - 7,000 liter gas cylinder (with CGA 580 valve)
Composition	Mixture 1: ^{129}Xe - 1Vol%; *N_2 - 10Vol%; He - 89Vol% (balance)* Mixture 2: ^{129}Xe - 3Vol%; *N_2 - 10Vol%; He - 87Vol% (balance)* ***For other compositions, please contact us.***

CO	≤ 1 ppm (mixtures) / ≤ 10 ppm (pure gas)
CO_2	≤ 1 ppm (mixtures) / ≤ 10 ppm (pure gas)
H_2O	≤ 1 ppm (mixtures) / ≤ 10 ppm (pure gas)
O_2	≤ 1 ppm (mixtures) / ≤ 10 ppm (pure gas)
THC	≤ 1 ppm (mixtures) / ≤ 5 ppm (pure gas)
CF_4	≤ 1 ppm (mixtures) / ≤ 5 ppm (pure gas)

Our Xenon-129 gas mixtures are manufactured in accordance with cGMP regulations.

Polarean Inc.

The 9820 ^{129}Xe hyperpolarizer provides a routine supply of high-purity, hyperpolarized ^{129}Xe for gas phase magnetic resonance studies. The polarizer is typically installed near the MRI/NMR suite and processes a custom mixture of ^{129}Xe, N_2, and ^{4}He, into one or more doses of pure hyperpolarized ^{129}Xe that is available for magnetic resonance studies. There is no chemical change associated with hyperpolarization – only nuclear spin alignment and cryogenic extraction of pure xenon. The hyperpolarized ^{129}Xe is then thawed and dispensed into a container or bag. Once dispensed into an appropriate container, and maintained within a modest holding magnetic field, the polarization relaxes with a T_1 of 1–2 hr.

The new generation 9820 xenon polarizer features a tunable 200W water-cooled narrowed linewidth laser, an expanded oven to accommodate substantially larger volume cells, and a 4-coil electromagnetic field configuration to provide uniform coverage over the oven and polarized gas plumbing.

System Overview and Specifications

The 9820 Xenon Hyperpolarization system can be operated on site by personnel who have undergone appropriate training. Polarization levels range over 35–45% depending on the volume and throughput of produced xenon, typically at 1–3 L/h. The system operates as a Class 1 laser, and thus requires no laser protective eyewear during normal operation.

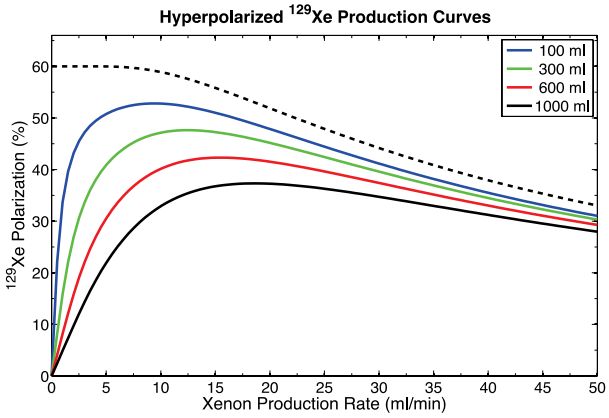

The 9820 xenon polarizer is capable of delivering ^{129}Xe polarization levels in the range of 35–45% as a function of production rate (1–3 L/h) when operating at the peak laser power. The dashed line shows the typical ^{129}Xe polarization leaving a 1.5-L cell whereas the color-coded lines depict the collected xenon volume using an effective solid-state xenon relaxation time of one hour.

Note: *The 9820 Xenon Hyperpolarization system is designed for research use. If the system is used to produce hyperpolarized ^{129}Xe for human inhalation, all applicable institutional and federal approvals must be obtained.*

The standard 9820 xenon polarizer configuration comes with a 1.5-L optical pumping cell, a triple-zone temperature control system, custom optics to deliver a highly uniform laser beam across the entire cell length, and a high efficiency cryogenic xenon collection system. The 9820 platform is designed with several expansion options to enhance performance and throughput as new components become available. In the picture above, oven and laser covers are removed to show the details.

System Components

- Custom hyperpolarized ^{129}Xe compatible valves and tubing
- Hyperpolarized ^{129}Xe collection plumbing within the electromagnetic field
- Narrowed linewidth tunable 200W 795-nm optical pumping laser in Class 1 housing
- Circular polarizing and beam collimating optics
- Mass flow and pressure transducers
- Closed circuit water chiller for robust temperature control
- High-field high-capacity cryogenic accumulation area
- Vacuum pump and purge function to prepare delivery containers
- Shielded oven with dual-action active heating/cooling temperature control
- Flow-through optical cell installed in series with rubidium pre-saturator each with its own dedicated temperature control
- Laser transmission and spectral monitoring
- Safety interlocks
- Central power distribution

Safety Features

- Filtered power distribution
- Air flow switch
- Interlocked protective laser housing for Class 1 operation
- CE Mark, UL and CSA approvals
- DOT approved shipping of replacement optical cells.

Optional Equipment and Services

- Polarization measurement station with absolute calibration for ^{3}He and ^{129}Xe
- Dual source ^{129}Xe cylinder manifold for real-time switching between natural abundance and enriched xenon mixes. This minimizes the risk of system contamination and downtime during frequent xenon cylinder changes.
- Heavy duty external purifier module with bypass function installed between the external gas manifold and the polarizer in order to further purify the gas mixes, protect the system against potential contamination and prolong the life of optical cells at their peak performance.
- Dose mixing syringes

Laboratory Space Requirements

- Controlled access space capable of temporary Class 4 laser operations
- Minimum room dimensions:
  - width 120" (3m)
  - depth 84" (2m)
  - height 84" (2m)
- Ferrous materials to be at least 3' (1m) away from the polarizer.
- Local ambient magnetic field preferably less than 1 Gauss

Polarizer Dimensions
170cm L x 60cm W x 160cm H
(65” L x 24” W x 60” H)

Electrical Requirements
- 3 phase 208 V, 47-63 Hz, 20 A per phase
- Power outlet: US NEMA L21-30R
- Lockable isolate box

Compressed Air
- 20 psig (1.5 bar) minimum pressure
- 4 standard cubic feet per minute (110 L/min) minimal flow
- 0.01% water maximal content

Environmental Requirements
- 5 kW/h maximal heat load (17,000 BTUH = 1.5 Ton)
- Room temperature between 68-75 ºF (20-24 ºC)
- Dedicated temperature control

Supplies and Consumables
- External ^{129}Xe-^{4}He-N_2 tank
- External UHP N_2 tank
- External commercial N_2 tank
- Liquid nitrogen
- Dose delivery bags

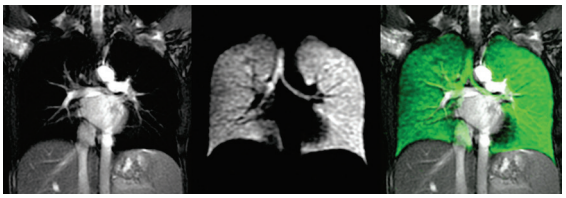

A pioneer in hyperpolarized gas systems, Polarean, Inc. is opening new avenues for functional and physiological imaging with its hyperpolarized gas MRI technology. High-resolution, 3D images of inhaled noble gases using conventional MRI scanners illuminate tissue characteristics and organ function currently inaccessible by existing methods. Hyperpolarized gases provide a promising research platform to extend MRI capabilities.

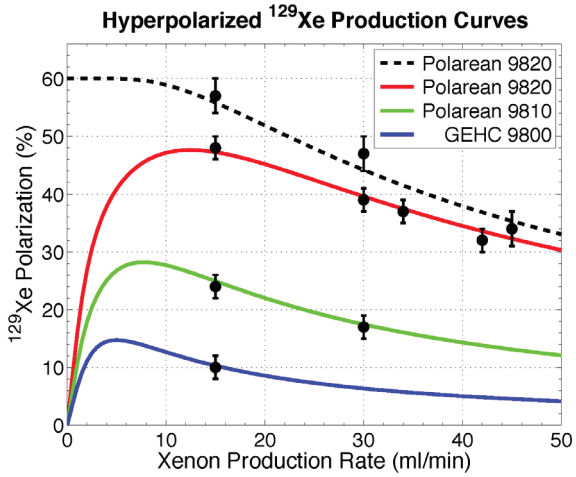

Predicted ^{129}Xe polarization level for a 300-ml batch after freeze-thaw as a function of flow for different polarizer generations Dashed line shows xenon polarization leaving the optical cell in 9820 polarizer using a 200W laser. Data point

PO Box 14805
Research Triangle Park, NC 27709-4805
United States
Phone: +1-(919)-206-7900
Fax: +1-(919)-206-7901
info@polarean.com

Nitrogen-15 in the form of gas and salts for medical and agricultural applications

Nitrogen-15 (^{15}N) is used to produce ^{15}N labelled chemical compounds. ^{15}N labelled chemical compounds are used for medical, biomedical and agriculture research. ^{15}N in the form of gas has the potential as a lung imaging agent due to its comparable properties to air.

Our Nitrogen-15 is available in the form of

- Nitrogen Gas
- Ammonium Chloride
- Ammonium Sulphate
- Potassium Nitrate
- Ammonium Nitrate

Enrichment	^{15}N > 99at%
Purity	> 99.9%
Volume (gas)	Available in various volumes and various valve connections (please contact us).
Packing (salts)	400g and 500g bottles

Oxygen-18 in the form of water for medical applications

Oxygen-18 is used to create tailored organochemical compounds labelled with the radio isotope ^{18}F (for example, 2-fluoro-2-deoxy glucose [^{18}FDG]). These are used for Positron Emission Tomography (PET), the latest cancer diagnostic technique.

Our Oxygen-18 is available in the form of water

Enrichment	^{18}O > 98at%, ^{17}O < 2at% ^{16}O < 2at%
Purity	> 99.9%
Volume	25g – 50g vials
Pyrogen	< 0.25 EU/ml
Conductivity	< 2 µS/cm
pH	6 – 8

Our Oxygen-18 products are manufactured in accordance with cGMP regulations and with the requirements of 21 Code of Federal Regulations: PARTS 210 and 211.

Our ISMRM Rubber Duck Family

Due to the great interest in our rubber ducks, we are pleased to introduce our rubber ducks from the previous ISMRM conferences.

The rubber ducks are not for sale and only available at our booth (#222).

Come and visit us to pick up your 2017 edition.

Nurse Xenia

Hawaii 2017 – 25th ISMRM

Nurse Gudrun

Singapore 2016 – 24th ISMRM

Dr. Willy

Toronto 2015 – 23rd ISMRM

Nurse Alberta

Salt Lake City 2013 – 21st ISMRM

Nurse Roberta

Melbourne 2012 – 20th ISMRM

Dr. Bob (Robert)

Montreal 2011 – 19th ISMRM

NUKEM Isotopes GmbH

Industriestr. 13
63755 Alzenau, Germany

T +49 (0)6023 91-1611
F +49 (0)6023 91-1614
E info@nukemisotopes.de

www.nukemisotopes.de